Check for updates

the plant journal

SEB SOCIETY FOR EXPERIMENTAL BIOLOGY

The Plant Journal (2023) **114,** 783–804 doi: 10.1111/tpj.16168

Deregulation of ζ-carotene desaturase in *Arabidopsis* and tomato exposes a unique carotenoid-derived redundant regulation of floral meristem identity and function

Ryan P. McQuinn[1], Julie Leroux[1], Julio Sierra[2], Lina Escobar-Tovar[2], Sarah Frusciante[3], E. Jean Finnegan[4], Gianfranco Diretto[3], Giovanni Giuliano[3], James J. Giovannoni[5], Patricia León[2,*] and Barry J. Pogson[1,*]

[1]*Australian Research Council Centre of Excellence in Plant Energy Biology, Research School of Biology, Australian National University, Canberra, ACT 2601, Australia,*

[2]*Departamento de Biología Molecular de Plantas, Instituto de Biotecnología, Universidad Nacional Autónoma de México, Av. Universidad 2001, Col. Chamilpa, Cuernavaca, Morelos 62210, Mexico,*

[3]*Italian National Agency for New Technologies, Energy, and Sustainable Development (ENEA), Casaccia Research Center, Rome 00196, Italy,*

[4]*CSIRO Agriculture and Food, Canberra, ACT 2601, Australia, and*

[5]*US Department of Agriculture-Agricultural Research Service, Robert W. Holley Center for Agriculture and Health, Ithaca, NY 14853, USA*

Received 1 March 2021; revised 5 February 2023; accepted 26 February 2023; published online 2 March 2023.
*For correspondence (e-mail patricia.leon@ibt.unam.mx; barry.pogson@anu.edu.au).

SUMMARY

A level of redundancy and interplay among the transcriptional regulators of floral development safeguards a plant's reproductive success and ensures crop production. In the present study, an additional layer of complexity in the regulation of floral meristem (FM) identity and flower development is elucidated linking carotenoid biosynthesis and metabolism to the regulation of determinate flowering. The accumulation and subsequent cleavage of a diverse array of ζ-carotenes in the *chloroplast biogenesis 5* (*clb5*) mutant of Arabidopsis results in the reprogramming of meristematic gene regulatory networks establishing FM identity mirroring that of the FM identity master regulator, APETALA1 (AP1). The immediate transition to floral development in *clb5* requires long photoperiods in a GIGANTEA-independent manner, whereas AP1 is essential for the floral organ development of *clb5*. The elucidation of this link between carotenoid metabolism and floral development translates to tomato exposing a regulation of FM identity redundant to and initiated by AP1 and proposed to be dependent on the E class floral initiation and organ identity regulator, SEPALLATA3 (SEP3).

Keywords: *Arabidopsis thaliana*, apocarotenoids, carotenoids, flower development, floral meristem identity, floral homeotic genes, retrograde signaling, *Solanum lycopersicum*.

INTRODUCTION

Establishing and maintaining floral meristem (FM) identity is paramount for plant reproductive success underpinning the production of fruits and grains that contribute to food security. Events leading to the emergence of the FM involve an elaborate reprogramming of gene regulatory networks in response to environmental factors (e.g. day length, abiotic stress) and endogenous cues, thereby driving the transition from a vegetative to a reproductive state (Andres & Coupland, 2012; Wils & Kaufmann, 2017). The timing of flowering with respect to season, environment and development is critical to the reproductive success of most plant species. Equally, the same fundamental variables impact photosynthesis and the allocation of energy and resources across the plant that is central for reproductive success. The development and physiological status of the chloroplast is communicated to the nucleus by a series of known and yet-to-be identified retrograde signaling cascades. We hypothesize that retrograde signaling provides a mechanism for an anticipated, but unresolved, coordination between photosynthetic organelles and meristem identity transitions.

The initiation of flowering in Arabidopsis is marked by major changes in gene transcription. Seasonal changes, such as day length and temperature, act via *GIGANTEA* (*GI*), *CONSTANS* (*CO*) and the epigenetic regulation of

© 2023 The Authors.
The Plant Journal published by Society for Experimental Biology and John Wiley & Sons Ltd.
This is an open access article under the terms of the Creative Commons Attribution-NonCommercial-NoDerivs License, which permits use and distribution in any medium, provided the original work is properly cited, the use is non-commercial and no modifications or adaptations are made.

FLOWERING LOCUS C (*FLC*) to initiate flowering (Andres & Coupland, 2012). Once the FM is initiated, establishing FM identity and subsequent floral development are heavily dependent on the activity of FM identity master regulatory transcription factors, *LEAFY* (*LFY*) and *APETALA1* (*AP1*) (Saddic et al., 2006; Pastore et al., 2011; Grandi et al., 2012; Wils & Kaufmann, 2017). Upon FM emergence, AP1 down-regulates several floral repressors from the APETALA2 (AP2) family of transcription factors (i.e. *SCHNARCHZAPFEN*, *SNZ*; *TARGET OF EAT1*, *TOE1*; and *TOE3*) (Kaufmann et al., 2010). In the early stages of FM development, AP1 also represses multiple floral promoting transcription factors (i.e. *AGAMOUS-like 24*, *AGL24*; *SUPPRESSOR OF CONSTANS1*, *SOC1*; *FLOWERING LOCUS D*, *FD*; and *FRUITFULL*, *FUL*), as well as *SHORT VEGETATIVE PHASE*, *SVP* and the *AP1*-antagonist *TERMINAL FLOWER 1* (*TFL1*), which are prevalent in the inflorescence meristem to promote the continuous emergence of floral primordia (Hanano & Goto, 2011; Kaufmann et al., 2010; Liljegren et al., 1999; Wigge et al., 2005). In doing so, AP1 establishes FM identity, maintaining its determinacy at the same time as securing its own expression for downstream floral organ speciation and development by inducing *LFY* via a positive feedback loop (Grandi et al., 2012). The repression of *SVP* and *AGL24* by AP1 relieves the negative regulation of *SEPALLATA3* (*SEP3*) (Pose et al., 2012) enabling AP1/SEP3 heterodimers to form and induce floral homeotic gene expression (*i.e. APETALA3*, *AP3* and *PISTILATA*, *PI*), ultimately initiating floral organ specification and development (Gregis et al., 2008; Wils & Kaufmann, 2017).

This establishment of FM identity is conserved across both monopodial (e.g. Arabidopsis and *Antirrhinum majus*, snapdragon) and sympodial (e.g. *Solanum lycopersicum*, tomato) dicots (Hong, 1998; MacAlister et al., 2012). In tomato, flower development research largely targets the maturation of the primary sympodial inflorescence meristem (SIM) governing the emergence of a secondary SIM prior to its own termination into a FM (MacAlister et al., 2012; Park et al., 2011). Within this SIM termination, understanding of FM identity regulation remains limited compared to Arabidopsis and Anthirrinum. However, *LFY* and *AP1* orthologues in tomato, *FALSIFLORA* (*FA*) and *MACROCALYX* (*MC*), respectively, play a role in establishing FM identity similar to LFY and AP1 and regulate tomato inflorescence complexity based on the observed reversion to a vegetative meristem in highly branched (or compound) secondary inflorescence shoots of null mutants *fa* and *mc-vin* (Molinero-Rosales et al., 1999; Yuste-Lisbona et al., 2016).

The four concentric whorls within the FM each give rise to one of four floral organs: sepals (whorl one), petals (whorl two), stamens (whorl three) and carpels (whorl four) (Krizek & Fletcher, 2005; Wellmer et al., 2014), according to the well-established ABCE model for flower development that describes the orchestrated interplay between floral homeotic transcription factors functioning in multimeric complexes within each whorl (Coen & Meyerowitz, 1991; Krizek & Fletcher, 2005; Wellmer et al., 2014). Whorl 1 identity (i.e. sepals) is controlled by the A-class genes *AP1* and *AP2*; whorl 2 identity (i.e. petals) is controlled by A- together with the B-class genes (*AP3* and *PI*), whorl 3 identity (i.e. stamens) is controlled by B-class genes and the C-class gene (*AGAMOUS*, *AG*), and whorl 4 identity (i.e. carpels) is controlled by *AG* (Bowman et al., 1991; Krizek & Fletcher, 2005). Additionally, the E-class *SEPALLATA* genes (*SEP1*, *SEP2*, *SEP3*, *SEP4*) as a whole are indispensable, functioning with a degree of redundancy in the multimeric complexes with A-, B- and C-class transcription factors, excluding AP2 (Ditta et al., 2004; Pelaz et al., 2000).

The loss of any one or combination of these floral homeotic transcription factors has drastic effects, resulting in the mis-development of leaf-like organs, loss of whorl specific floral organs and/or repetitive floral organ development in several whorls (Bowman et al., 1991; Ditta et al., 2004; Pelaz et al., 2000). Yet, although these regulatory networks have been well characterized, the potential contribution of plant-derived metabolic signals aiding in the timing and irreversible transition from shoot apical meristem to the FM remains largely unexplored (Chandler, 2012).

Plants respond to environmental fluctuations by altering their physiological state, using hormones and cellular signals. Plants have evolved diverse (in the order of dozens) chloroplast-to-nucleus retrograde cellular signals affecting the expression of thousands of genes that detoxify free radicals, repair damage and allow better acclimatization of the cell (Chan et al., 2016). These retrograde signals include, but are not limited to, reactive oxygen species (ROS) such as singlet oxygen ($^1O_2$) and hydrogen peroxide (H_2O_2), SAL1-PAP, oxyphytodienoic acid, dihydroxyacetone phosphate, β-cyclocitral and β-cyclocitric acid (Chan et al., 2016; D'Alessandro et al., 2019; Ramel et al., 2012). The latter two retrograde signals originate from the same set of metabolites (i.e. carotenoids) that produce the essential phytohormones, ABA and strigolactone (D'Alessandro et al., 2019; Ramel et al., 2012).

In addition to modulating and communicating chloroplast homeostasis, retrograde signaling enables the chloroplast to function as an environmental sensor for the cell and adjust plant development (Chan et al., 2016). Of particular interest is the link between carotenoid biosynthesis and metabolism and regulation of plant development. Accumulation of apocarotenoid signals originating in the chloroplast via enzymatic and non-enzymatic carotenoid cleavage by carotenoid cleavage dioxygenases (CCDs) and ROS, respectively, has been linked to the regulation of nuclear gene transcription. These transcriptional modulations are

© 2023 The Authors.

1365313x, 2023, 4, Downloaded from https://onlinelibrary.wiley.com/doi/10.1111/tpj.16168 by E.N.E.A., Wiley Online Library on [09/02/2024]. See the Terms and Conditions (https://onlinelibrary.wiley.com/terms-and-conditions) on Wiley Online Library for rules of use; OA articles are governed by the applicable Creative Commons License

the result of retrograde signaling cascades initiated by apocarotenoid signals, for which most of the intermediate signaling components of remain to be determined, and they impact various aspects of vegetative plant development (e.g. leaf and root development, and skoto- and photo-morphogenesis) (Avendaño-Vázquez et al., 2014; Cazzonelli et al., 2020; Dickinson et al., 2019; Jia et al., 2019; Wang et al., 2019). Yet, it remains to be determined whether chloroplast homeostasis and communication may impact the similarly resource intensive processes of reproductive development.

The poly-*cis*-transformation of 15-*cis*-phytoene to *all trans*-lycopene early in carotenogenesis has garnered increased attention as a potential source of apocarotenoid signals affecting aspects of plant development. In bacterial carotenogenesis 15-*cis*-phytoene is converted to *all trans*-lycopene through six chemical transformations carried out by a single enzyme, CRTI. Through evolution, plants have evolved a more complex poly-*cis*-transformation pathway providing more control points (i.e. genes) that the plant can transcriptionally regulate in a tissue and developmental stage specific manner (Figure 1a). The reactions are as

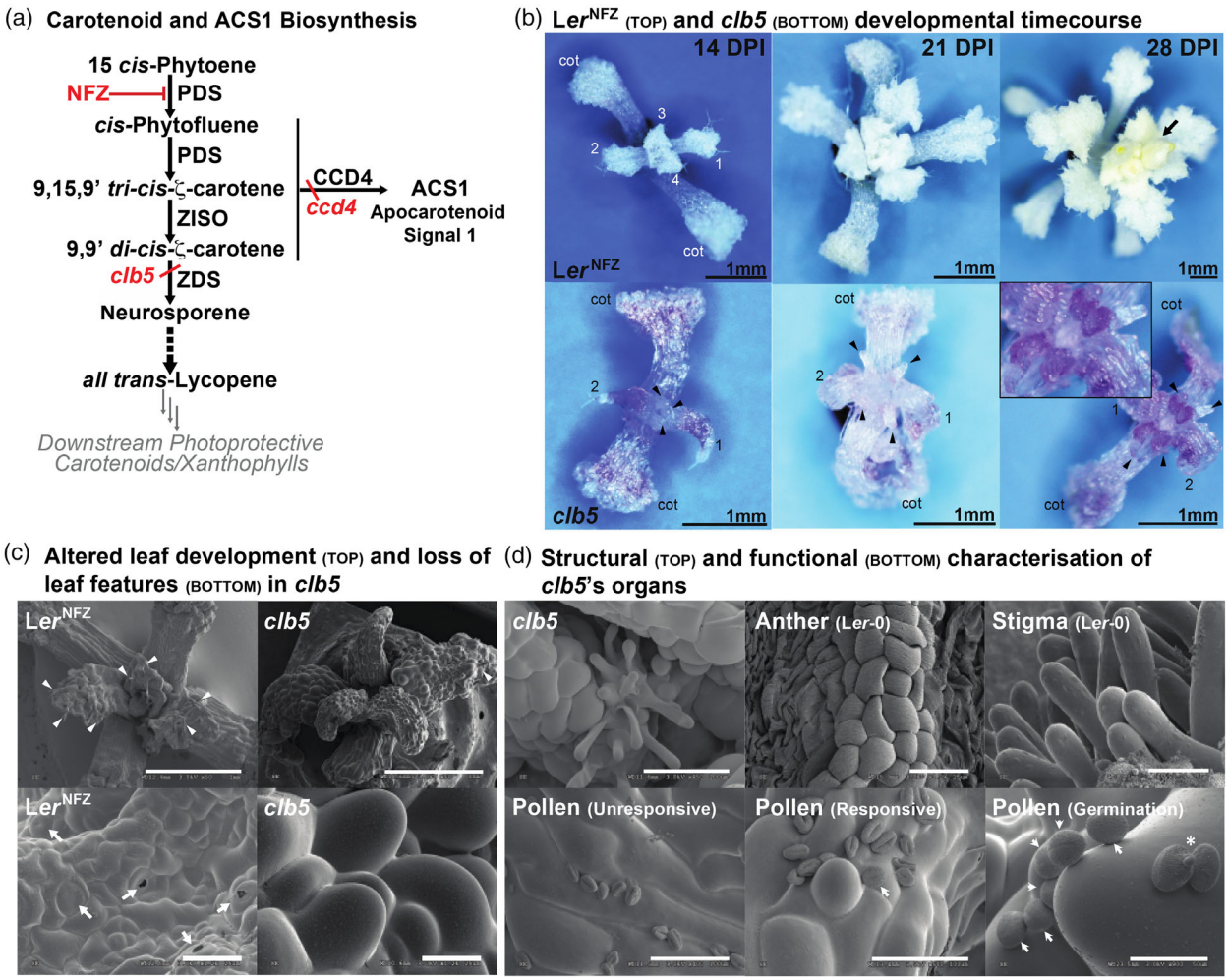

Figure 1. The *clb5* mutation in ZDS of Arabidopsis manifests in a determinate meristem from which chimeric floral organs arise.
(a) Simplified carotenoid biosynthetic pathway describing the poly-*cis* transformation of 15 *cis*-phytoene to *all trans*-lycopene, preceding the synthesis of photoprotective carotenes and xanthophylls, including the proposed biosynthesis of ACS1 according to Avendaño-Vázquez et al. (2014). Enzymes are shown in bold. PDS, phytoene desaturase; ZISO, zeta-carotene isomerase; ZDS, zeta-carotene desaturase; CRTISO, carotenoid isomerase; CCD4, carotenoid cleavage dioxygenase 4. *clb5* and *ccd4* mutations are denoted in red italics. Norflurazon (NFZ) is a chemical inhibitor of PDS.
(b) Developmental phenotypes of Ler^{NFZ} (TOP) and *clb5* (BOTTOM) seedlings at 14, 21 and 28 DPI. Inflorescence and developing floral buds on Ler^{NFZ} plants are indicated with an arrow. 'cot' indicates cotyledons and leaves are numbered. Chimeric floral organs are indicated by arrowheads.
(c) Cryo-SEM images comparing shoot apical meristem and leaf development in the albino control, Ler^{NFZ} and *clb5* seedlings. Scale bars = 1 mm (top) and 25 μm (bottom). Trichomes and stomata are indicated by arrowheads and arrows, respectively.
(d) Top: Cryo-SEM images comparing cell morphologies of *clb5* chimeric floral organs (scale bar = 100 μm) and their similarity to that of anthers (scale bar = 25 μm) and stigmatic cells (scale bar = 25 μm) from L*er*-0 flowers. Additional floral tissues are shown in Figure S3. Bottom: Cryo-SEM images showing functionality of stigmatic papillae of *clb5*. Scale bars in order = 100 μm, 100 μm and 50 μm. Swelling and germinating pollen grains are indicated with arrows and asterisk, respectively (see also Figures S1 and S3).

© 2023 The Authors.

1365313x, 2023, 4, Downloaded from https://onlinelibrary.wiley.com/doi/10.1111/tpj.16168 by E.N.E.A., Wiley Online Library on [09/02/2024]. See the Terms and Conditions (https://onlinelibrary.wiley.com/terms-and-conditions) on Wiley Online Library for rules of use; OA articles are governed by the applicable Creative Commons License

follows: 15-*cis*-phytoene is desaturated twice by phytoene desaturase (PDS) generating 9,15,9′-*tri-cis*-ζ-carotene; 9,15,9′-*tri-cis*-ζ-carotene is isomerized by ζ-carotene isomerase (ZISO) producing 9,9′-*di-cis*-ζ-carotene; ζ-carotene desaturase (ZDS) desaturates 9,9′-*di-cis*-ζ-carotene twice providing 7,9,7′9′-*tetra-cis*-lycopene, which is subsequently isomerized by carotenoid isomerase (CRTISO) to give *all trans*-lycopene (McQuinn et al., 2020). These multiple control points are considered to provide plants the opportunity to accumulate carotene intermediates in the poly-*cis*-transformation pathway when developmentally required, the subsequent cleavage of which produces apocarotenoids that initiate retrograde signaling cascades, ultimately providing an additional means to regulate plant development through transcriptional reprogramming (Sierra et al., 2022).

Therefore, examining mutants within the poly-*cis*-transformation pathway, including albino mutants, incapable of photosynthesizing, provides a unique opportunity to explore potential links between the accumulation and subsequent cleavage of acyclic carotene intermediates with the regulation of various aspects of plant development. Although using albino mutants to discover and characterize signals may appear to be counterintuitive when studying plant developmental biology, it is important to note that there are key cell types and tissues (e.g. deep within the shoot apical meristem and roots, respectively) containing undifferentiated plastids or non-photosynthetic plastids essential for plant development (Liebers et al., 2017). Furthermore, normal plant development of albino carotenogenic mutants can be achieved when a carbon source (i.e. sucrose) is supplemented, providing a mechanism to perturb flux and thereby reveal roles for (apo)carotenoids.

Characterization of the Arabidopsis *ccr2* mutant disrupting *CRTISO* has linked CRTISO carotene substrate-derived apocarotenoids to the regulation of skotomorphogenesis (Cazzonelli et al., 2020). The resulting undefined apocarotenoid(s) in *ccr2* initiates transcriptional reprogramming in parallel with DEETIOLATED1 (DET1), a repressor of photomorphogenesis, supporting the above hypothesis (Cazzonelli et al., 2020). Additionally, the *chloroplast biogenesis 5* (*clb5*) mutant in Arabidopsis containing a lesion in *ZDS* displays profound alterations in leaf morphology and cellular differentiation suggesting deregulation of meristematic function (Avendaño-Vázquez et al., 2014) (Figure 1a,b). Indeed, over-accumulation of ZDS substrates and subsequent cleavage by CCD4 initiates a retrograde signaling cascade that represses nuclear-encoded chloroplast-targeted ribosomal subunits, thereby inhibiting chloroplast translation (Avendaño-Vázquez et al., 2014; Escobar-Tovar et al., 2020; Hou et al., 2016). This loss of chloroplast translation results in altered leaf development producing radial leaves (Escobar-Tovar et al., 2020).

In the present study, we provide evidence that the accumulation of ZDS substrates and their subsequent cleavage in the *clb5* mutant is capable of driving a massive reprogramming of gene regulatory networks associated with FM identity within the shoot apical meristem, ultimately converting it to a determinate FM. This unique conversion is dependent on long day (16:8 h light/dark) conditions in a GI-independent manner, with AP1 being exclusively required for subsequent chimeric floral organ development. In further support of this result, we demonstrate that *ZDS* is uniquely regulated during early stages of flower development when FM identity is established under indirect control of the FM identity master regulator AP1. Lastly, we confirm that removal of the ζ-carotene-derived apocarotenoid signal through the constitutive over-expression *ZDS* impairs floral meristem termination in tomato.

RESULTS

The *clb5* mutation in *ZDS* manifests in altered meristem function and development of chimeric floral organs

Upon investigating the development of Arabidopsis albino carotenogenic mutants within and preceding the poly-*cis*-transformation pathway, we demonstrated that the *ZDS* mutation, *clb5*, manifests in seedlings that are unique among other albino carotenogenic mutants forming radial primary leaves and ceasing further development (Avendaño-Vázquez et al., 2014). By modifying tissue culture media with an increased carbon source, we prolonged the growth of *clb5* seedlings beyond our earlier reports (Figure 1a,b) (Avendaño-Vázquez et al., 2014; Escobar-Tovar et al., 2020). Under these conditions, wild-type Landsberg *erecta* seedlings treated with norflurazon (L*er*^{NFZ}), an herbicide that blocks carotenogenesis by inhibiting phytoene desaturase activity, develops leaves similarly to that of wild-type, producing numerous lamellar leaves with trichomes, stomata, and normal phyllotaxy (Figure 1b,c). Further, L*er*^{NFZ} seedlings successfully transitioned to reproductive development with complete flowers emerging from the rosette around 21 days post imbibition (DPI) (Figure 1b and Figure S1), consistent with wild-type development under long photoperiods. It is significant that L*er*^{NFZ} and all other examined albino carotenogenic mutants do not show major aberrations in seedling development as exhibited by disrupting ZDS within the carotenoid biosynthesis. Consequently, L*er*^{NFZ} represents the best albino control, opposed to *pds3*, because it does not display altered plant development resulting from feedback inhibition of gibberellic acid biosynthesis. Thus, this provides an optimal opportunity to explore the developmental alterations specific to the *clb5* mutant, distinct from the shared impairment of photosynthesis and carotenoid derived hormones (i.e. strigolactones and ABA) (Qin et al., 2007).

© 2023 The Authors.

1365313x, 2023, 4, Downloaded from https://onlinelibrary.wiley.com/doi/10.1111/tpj.16168 by E.N.E.A., Wiley Online Library on [09/02/2024]. See the Terms and Conditions (https://onlinelibrary.wiley.com/terms-and-conditions) on Wiley Online Library for rules of use; OA articles are governed by the applicable Creative Commons License

By contrast to L*er*^{NFZ}, *clb5* seedlings display significantly altered meristematic function (Figure 1). After development of the primary radial leaves, at approximately 14 DPI, the *clb5* shoot apical meristem transitions to a determinate meristem from which three to four needle-like organs develop (Figure 1b,c). These needle-like organs have significantly reduced numbers of trichomes and stomata and emerge simultaneously in a whorled arrangement (Figure 1c). No further development was observed in *clb5* seedlings once these organs emerged (Figure 1b). Importantly, the developmental aberrations in *clb5* were not reverted by exogenous gibberellic acid application, in contrast to the observed dwarf phenotype reversion of *pds3*, further supporting the unique association of this altered development to the deficiency of ZDS (Figure S2).

The determinate nature of the meristem and whorled arrangement of the needle-like organs share striking similarities with that of the floral meristem and flower development. Cryogenic scanning electron microscopy (cryo-SEM) was employed to investigate the morphological characteristics of the needle-like organs, comparing their epidermal cell shape and structure to distinct cell types present in wild-type leaves and floral tissues (Figure 2d; Figure S3a). The epidermal cells of the needle-like organs of *clb5* are a mosaic of two different cell types, one of them with morphological features resembling anther cells of the stamen, and the other elongated similar to stigmatic papillae of the carpel (Figure 1d; Figure S3a).

To further explore the physiological functionality of the stamen-like and stigmatic papillae-like cells, mature pollen grains from L*er*-0 were brushed on *clb5* needle-like organs and incubated for 24 h (Figure 1d). Pollen grains remained unresponsive unless in contact with protruding cells resembling stigmatic papillae on *clb5* needle-like organs (Figure 1d). When in contact with these cells, the

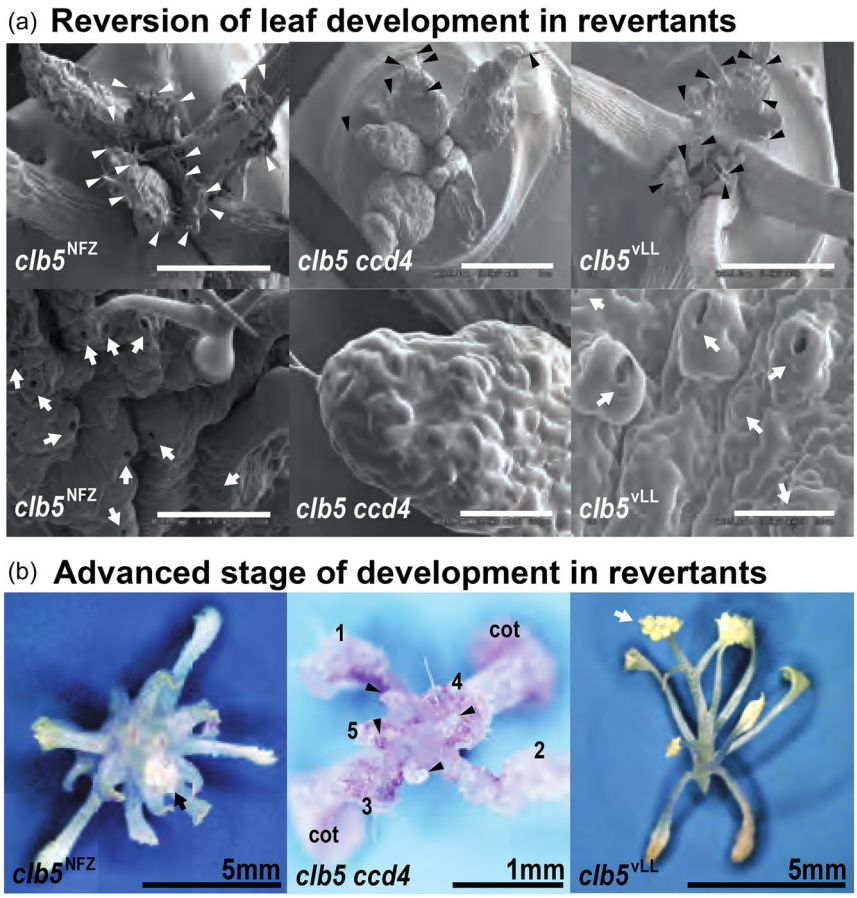

Figure 2. Aberrant meristem function in *clb5* is associated with over-accumulation and subsequent cleavage of ζ-carotenes.
(a) Cryo-SEM images showing the reversion of *clb5* phenotypes when grown on NFZ, *clb5*^{NFZ} (scale bars = 1 mm and 100 μm), *clb5 ccd4* (scale bars = 1 mm and 25 μm) and grown under low light (< 10 μmol m^{-2} sec^{-1}), *clb5*^{vLL} (scale bars = 1 mm and 100 μm). Stomata and trichomes are indicated by arrows and arrowheads, respectively.
(b) Images of 28 DPI seedlings demonstrating phenotype reversion in *clb5*^{NFZ} (scale bar = 5 mm), *clb5 ccd4* (scale bar = 1 mm) and *clb5*^{vLL} (scale bar = 5 mm). Developing florets on *clb5*^{NFZ} and *clb5*^{vLL} plants are identified with an arrow. *clb5 ccd4* cotyledons are indicated by 'cot', lamellar leaves are numbered (1–5) and chimeric floral organs are identified with arrowheads.

© 2023 The Authors.

1365313x, 2023, 4, Downloaded from https://onlinelibrary.wiley.com/doi/10.1111/tpj.16168 by E.N.E.A., Wiley Online Library on [09/02/2024]. See the Terms and Conditions (https://onlinelibrary.wiley.com/terms-and-conditions) on Wiley Online Library for rules of use; OA articles are governed by the applicable Creative Commons License

pollen grains swelled, with some eventually germinating, demonstrating that these cells behave as functional stigmatic papillae (Figure 1d). Combined, these results suggest the pollen grain response is specific to contact with the stigmatic papillae-like cells, and not a result of changes in relative humidity. Given the pronounced development of carpelloid stigmatic papillae-like cells on the needle-like organs, histochemical GUS assays were carried out to further characterize their molecular identity and the needle-like organs on which they reside. Specific reporters to stigma (YJ-STIG::GUS, Figure S3b–e) and style tissues (SHP1::GUS, Figure S3f–i) of Arabidopsis carpel, as previously described in Alvarez et al. (2009), were introduced into the *clb5* background. YJ-STIG::GUS expression throughout the *clb5* needle-like organs confirms the molecular identity of these unique cells as stigmatic papillae-like (Figure S3c), whereas the lack of SHP1::GUS expression shows the absence of additional features consistent with carpel identity (Figure S3g).

Collectively, these results indicate that the needle-like organs of *clb5* are chimeric floral organs with stamenoid (anther cells) and carpelloid (stigmatic papillae) developmental features, and therefore will be referred to hereafter as chimeric floral organs.

Aberrant meristem function in *clb5* is linked to ζ-carotene over-accumulation and subsequent cleavage

Formation of the radial primary leaves in *clb5* is a result of the synthesis of unidentified apocarotenoids upon cleavage of ζ-carotenes by CCD4 (Avendaño-Vázquez et al., 2014). Given that, we investigated whether the development of the chimeric floral organs and the determinate meristem of *clb5* are similarly regulated by inhibiting the synthesis of ζ-carotenes using NFZ, as well as ζ-carotene-derived apocarotenoid synthesis by removing CCD4.

First, HPLC enabled the accurate identification and quantification of carotenes accumulating in *clb5*. As previously reported, in green leaves of L*er*-0, carotenes within the poly-*cis*-transformation of 15 *cis*-phytoene to *all trans*-lycopene (e.g. phytoenes, phytofluenes, and ζ-carotenes) are undetectable (data not shown) (Qin et al., 2007). However, in contrast to wild-type, the loss of ZDS results in the significant accumulation of not one but 19 distinctive ζ-carotene isomers in *clb5* seedlings at 14 DPI, 12 of which were further defined. Four represent the most commonly quantified in plant tissues (i.e. 9,15,9′-*tri-cis*-ζ-carotene, 9,9′-*di-cis*-ζ-carotene, 9-*cis*-ζ-carotene and *all trans*-ζ-carotene) (Table 1; Figure S4). The eight remaining ζ-carotenes have been confirmed to be ζ-carotene isomers based on their UV spectrum and mass-to-charge ratio via LC coupled with atmospheric pressure chemical ionization high-resolution mass spectrometry (APCI-HRMS) (Table S1; Figure S5).

As expected, accumulation of ζ-carotene isomers in *clb5* seedlings was inhibited upon transfer to NFZ supplemented media (*clb5*^{NFZ}) because it blocks the enzymatic activity in the preceding step in the pathway (PDS), resulting in accumulation of phytoene (Table 1). Only three of the ζ-carotene isomers identified in the *clb5* mutant were detectable (9,9′-*di-cis*-ζ-carotene, 9-*cis*-ζ-carotene and *all trans*-ζ-carotene), albeit at significantly lower levels (Table 1). The reduction in ZDS substrates coincided with reversion of the leaf and floral phenotypes of *clb5*^{NFZ} seedlings, including lamellar leaves with spiral phyllotaxy, exhibiting trichomes and stomata, instead of determinate whorls of chimeric floral organs (Figure 2a). Furthermore, 50–60% of *clb5*^{NFZ} plants subsequently transitioned to L*er*^{NFZ}-like reproductive development by 28 DPI (Figure 2b).

Introduction of the *ccd4* mutation in *clb5* significantly increased 10 of the 19 detectable ζ-carotene isomers and 15-*cis*-phytoene (Table 1). This accumulation within the carotenoid profile is consistent with the idea that the loss of CCD4 results in reduced enzymatic cleavage of specific ζ-carotene isomers and 15-*cis*-phytoene. The altered carotenoid profile in *clb5 ccd4* was also morphologically associated with the formation of lamellar primary leaves with increased numbers of trichomes and stomata consistent with previous reports (Figure 2a) (Avendaño-Vázquez et al., 2014). Furthermore, development in *clb5 ccd4* plants post primary leaves was also temporarily restored with the next three or four leaves displaying a lamellar shape similar to L*er*^{NFZ} (Figure 2a,b). However, after the emergence of leaf four or five in *clb5 ccd4* plants, three or four chimeric floral-like organs emerge from the converted floral-like meristem similar to that observed in *clb5*, suggesting *ccd4* delays, rather than fully reverts, the development of chimeric floral organs in *clb5* (Figure 2b).

The transient reversion in *clb5 ccd4* also supports the potential for non-enzymatic cleavage of ζ-carotene isomers by singlet oxygen ($^1O_2$) as a consequence of light exposure during later developmental stages (Escobar-Tovar et al., 2020). To further support this *clb5* seedlings were grown under very low light conditions (< 10 μmol m^{-2} sec^{-1}) (*clb5*^{vLL}) (Table 1 and Figure 2a,b). The very low light growth condition broadly affected the carotenoid profile in *clb5* by increasing all carotenoids, ranging from six-fold for ζ-carotene isomer 2 to 106-fold for ζ-carotene isomer 5 (Table 1). Very low light also reverted the developmental phenotypes such that *clb5*^{vLL} seedlings closely resembled L*er*^{NFZ} (Escobar-Tovar et al., 2020). Furthermore, this reversion is maintained through to the transition to reproductive development at 28 DPI (Figure 2a,b).

Together, these data suggest that the floral phenotypes in *clb5* seedlings are associated with an over-accumulation and subsequent cleavage of ζ-carotene isomers in a CCD4- and light-dependent manner.

© 2023 The Authors.

1365313x, 2023, 4, Downloaded from https://onlinelibrary.wiley.com/doi/10.1111/tpj.16168 by E.N.E.A., Wiley Online Library on [09/02/2024]. See the Terms and Conditions (https://onlinelibrary.wiley.com/terms-and-conditions) on Wiley Online Library for rules of use; OA articles are governed by the applicable Creative Commons License

Table 1 Carotenoid content of *clb5* revertants compared to *clb5* (ng g^{-1} FW, $n = 3$) (mean ± SE)

				clb5 revertants	
Carotenoids	UV Spectrum	*clb5*	*clb5*^{NFZ}	*clb5;ccd4*	*clb5*^{vLL}
286 nm (*Abs*^{max})					
15 *cis*-phytoene	276, 286, 298	ND	**4221.86 ± 449.07**	**92.38 ± 13.28**	**440.74 ± 51.56**
Phytoene 2	276, 286, 298	ND	**1360.90 ± 146.18**	ND	ND
348 nm					
Phytofluene 1	332, 348, 368	ND	**7.62 ± 0.93**	ND	**152.87 ± 27.76**
Phytofluene 2	332, 348, 368	ND	**9.61 ± 1.04**	ND	**126.68 ± 35.36**
400 nm					
ζ-carotene isomer 1[b]	(296) 378, 400, 424	ND	ND	ND	**37.37 ± 5.42****
ζ-carotene isomer 2[b]	378, 400, 424	8.85 ± 0.82	ND	**12.31 ± 0.11***	**119.48 ± 38.59***
ζ-carotene isomer 3[b]	378, 400, 424	20.65 ± 0.52	ND	**27.29 ± 1.13****	**116.36 ± 11.75****
ζ-carotene isomer 4[b]	(290) 378, 400, 424	7.54 ± 1.57	ND	10.55 ± 1.00	**108.95 ± 30.40***
ζ-carotene isomer 5[a,b]	(292) 378, 400, 424	2.35 ± 2.35	ND	10.26 ± 1.57	**249.82 ± 14.99*****
9,15,9′ *tri-cis*-ζ-carotene[a,b]	(296) 376, 396, 422	19.85 ± 0.29	ND	**14.76 ± 1.12***	**315.45 ± 19.04*****
ζ-carotene isomer 7[a,b]	(296) 376, 396, 422	12.80 ± 0.92	ND	17.68 ± 2.51	**334.65 ± 31.38*****
ζ-carotene isomer 8[a,b]	(296) 376, 396, 422	7.23 ± 0.55	ND	11.22 ± 2.10	**75.62 ± 4.65*****
ζ-carotene isomer 9[b]	(296) 376, 396, 422	5.79 ± 0.51	ND	7.72 ± 0.02	**147.74 ± 7.69*****
9,9′ *di-cis*-ζ-carotene[a,b]	(294) 380, 400, 426	56.67 ± 6.39	**8.25 ± 1.83*****	**114.55 ± 13.02***	**2103.16 ± 133.48*****
9 *cis*-ζ-carotene[a,b]	(294) 380, 400, 426	50.82 ± 3.01	**13.41 ± 0.45*****	**89.81 ± 9.15***	**1592.31 ± 26.50*****
All trans-ζ-carotene[a,b]	(294) 380, 400, 426	13.09 ± 0.72	**6.29 ± 0.72***	**19.46 ± 1.64***	**434.47 ± 30.38*****
ζ-carotene 13	(294) 378, 398, 422	6.65 ± 0.79	ND	8.67 ± 0.18	**48.49 ± 2.33*****
ζ-carotene 14	(296) 380, 400, 426	13.59 ± 0.47	ND	**21.28 ± 1.93***	**185.35 ± 10.10*****
ζ-carotene 15	(292) 380, 400, 426	18.78 ± 1.01	ND	**31.00 ± 2.50***	**309.29 ± 8.95*****
ζ-carotene 16	(294) 380, 400, 426	9.27 ± 0.83	ND	**14.60 ± 1.29***	**149.38 ± 3.85*****
ζ-carotene 17	(296) 380, 400, 426	17.15 ± 2.12	ND	23.90 ± 1.56	**143.68 ± 11.52*****
ζ-carotene 18	(296) 380, 400, 426	16.17 ± 0.87	ND	**25.71 ± 1.61****	**144.71 ± 4.79*****
ζ-carotene 19	(296) 382, 400, 426	7.27 ± 0.86	ND	**12.52 ± 0.17****	**62.90 ± 3.14*****

ND indicates carotenoids that were below the limits of detection give the current analytical conditions.
Statistically significant changes in carotenoid amount compared to *clb5* are indicated in bold. Statistical analysis was performed using Student's *t*-test with the results shown as: *$P < 0.05$; **$P < 0.01$; ***$P < 0.001$).
Shaded rows indicate newly identified ζ-carotene isomers in *clb5*.
(see also Figures S4 and S5; Table S1).
[a]ζ-carotene isomers previously identified in tomato (Fantini et al., 2013; McQuinn et al., 2020).
[b]Carotenoid identification confirmed as ζ-carotene isomers according to m/z ratio via LC-APCI-MS.

Massive reprogramming of gene regulatory networks associated with floral meristem identity and organ development underpins the aberrant meristem function in *clb5*

During flowering in the monopodial Arabidopsis, the vegetative meristem is transformed first into an inflorescence meristem from which floral meristems emerge and develop into a complete flower. The early formation of chimeric floral organs after the first set of true leaves raises the question as to which meristem maintenance and FM identity genes are deregulated consequent to the over-accumulation and subsequent cleavage of ZDS carotene substrates. This was investigated using meristem-enriched samples of seedlings at 14 DPI, representing the time when chimeric floral organs just begin to emerge in *clb5* (Figure 3).

Primary alterations in the meristem homeostasis of *clb5* are evident in the massive induction of meristem maintenance genes, *WUS* and *CLV3* in *clb5* compared to L*er*^{NFZ} (Figure S6a). *WUS* was induced by 32-fold relative to L*er*^{NFZ}, whereas *CLV3* was induced by 10-fold (Figure S6a). Interestingly, although histochemical GUS assays demonstrate *CLV3* expression covers a broader area in the upper layers of the *clb5* meristem, coinciding with an apparent enlarged meristem, *WUS* expression is relocated from deep within the meristem to the tips of the chimeric floral organs of *clb5* (Figure S6b,c).

Regarding floral development, transcript abundance of AP2-like floral repressors (i.e. *AP2*, *SMZ*, *SNZ*, and *TOE1*, *2* and *3*), floral promoters (i.e. *AGL24*, *SOC1*, *FD* and *FUL*), transcription factors maintaining the indeterminate nature of the shoot apical and inflorescence meristems (i.e. *SVP* and *TFL1*) and floral homeotic transcription factors (i.e. *AP1*, *AP3*, *PI*, *AG*, and *SEP1*, *2* and *3*) were quantified in *clb5* relative to L*er*^{NFZ} in a primary comparison (Figure 3). Three of the six AP2-like floral repressors, *SNZ*, *TOE1* and

© 2023 The Authors.

1365313x, 2023, 4, Downloaded from https://onlinelibrary.wiley.com/doi/10.1111/tpj.16168 by E.N.E.A., Wiley Online Library on [09/02/2024]. See the Terms and Conditions (https://onlinelibrary.wiley.com/terms-and-conditions) on Wiley Online Library for rules of use; OA articles are governed by the applicable Creative Commons License

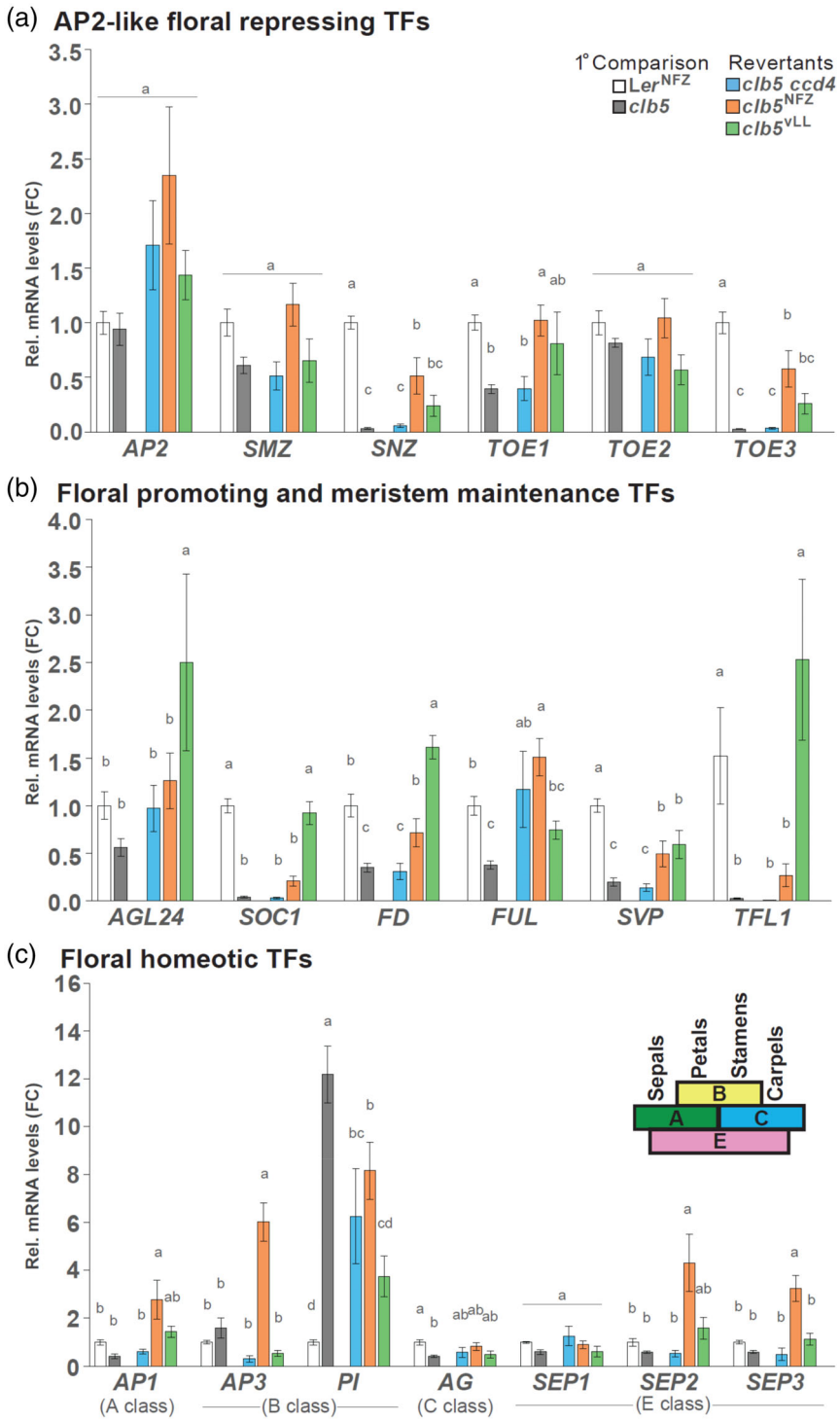

Figure 3. Reprogramming of gene regulatory networks involved in FM identity and floral organ development.
(a) AP2-like floral repressor mRNA levels relative to the albino control L*er*^{NFZ}.
(b) Shoot apical meristem identity and floral development regulator mRNA levels relative to L*er*^{NFZ}.
(c) Floral homeotic transcription factor mRNA levels relative to L*er*^{NFZ}.
In all experiments $n \geq 4$, each in triplicate. Statistical significance was determined based on FDR <0.05. Inset is a visual depiction of the ABCE model coordinating gene class with floral organ development. Data are represented as the mean ± SEM from three independent biological replicates (see also Figure S5).

© 2023 The Authors.

1365313x, 2023, 4, Downloaded from https://onlinelibrary.wiley.com/doi/10.1111/tpj.16168 by E.N.E.A., Wiley Online Library on [09/02/2024]. See the Terms and Conditions (https://onlinelibrary.wiley.com/terms-and-conditions) on Wiley Online Library for rules of use; OA articles are governed by the applicable Creative Commons License

TOE3, were strongly repressed in *clb5* compared to L*er*^{NFZ}, with *SNZ* and *TOE3* significantly repressed by 97% and *TOE1* repressed by 62% (Figure 3a). Five of the six floral-promoting and meristem maintenance transcription factors analyzed were significantly repressed by greater than 50% in *clb5* seedlings compared to L*er*^{NFZ}, with *SOC1*, *SVP* and *TFL1* repressed by 96, 80 and 90%, respectively (Figure 3b). The expression of the MADS-box transcription factors from the ABCE model of floral whorl identity and organ initiation was significantly deregulated in the *clb5* seedlings, with the largest impact being a 14-fold induction of the B-class gene *PI* (Figure 3c). Expression of the C-class gene *AG* was also affected in *clb5*, but to a lesser extent, being repressed by 57% relative to L*er*^{NFZ} (Figure 3c). It is important to note that transcripts for all floral homeotic genes, apart from *SEP4*, were detected and quantified in each genotype and condition tested (Figure 3c).

Consistent with the partial phenotypic reversion observed in *clb5 ccd4*, the absence of CCD4 results in modest reversion to the altered expression profile of *clb5* (Figure 3; Figure S6a). The expression of both *WUS* and *CLV3* in *clb5 ccd4* reverted to levels comparable to L*er*^{NFZ} (Figure S6a), although the AP2-like transcription factors remained repressed similar to *clb5* (Figure 3a). Among the three floral promoters (i.e. *SOC1*, *FD*, and *FUL*) and two meristem maintenance factors (*SVP* and *TFL1*) repressed in *clb5*, only *FUL* expression returned to levels comparable to the albino control in *clb5 ccd4* (Figure 3b). For the floral homeotic genes, *PI* and *AG*, there was significant, albeit intermediate, reversion in *clb5 ccd4* (Figure 3c).

Consistent with the developmental reversion (Figure 3) mediated by NFZ and very low light treatments, gene expression levels were restored in *clb5*^{NFZ} treatments for all but two transcription factors (Figure 3), whereas 100% of floral regulatory genes were restored in the *clb5*^{vLL} towards levels similar to or higher than those observed in L*er*^{NFZ} (Figure 3). Significant increases in the expression of the floral repressing transcription factors *SNZ*, *TOE1* and *TOE3* towards that of L*er*^{NFZ} were observed in *clb5*^{NFZ} and *clb5*^{vLL}, albeit to varying degrees (Figure 3a). In *clb5*^{NFZ}, mRNA levels for the floral promoters *FD* and *FUL* returned to levels similar to or higher than L*er*^{NFZ}, respectively (Figure 3b). Concurrently, the meristem maintenance factor *SVP* transcripts increased significantly, but remained less than L*er*^{NFZ} (Figure 3b). The transcripts for *SOC1* and *TFL1* in *clb5*^{NFZ} increased compared to *clb5*, yet narrowly fell short of the significance threshold [i.e. false discovery rate (FDR) < 0.05] (Figure 3b).

Out of all genetic and environmental revertant treatments tested, *clb5*^{vLL} showed the strongest reversion with respect to mRNA levels for all of the five flower-promoting and meristem maintenance transcription factors deregulated in *clb5*, returning to levels recorded in L*er*^{NFZ}, or higher in the case of *FD* (Figure 3b). *clb5*^{vLL} has significant recovery of *PI* expression in the direction of L*er*^{NFZ} (Figure 3c). Regarding the *AG* gene, both *clb5*^{NFZ} and *clb5*^{vLL} showed increased expression similar to that of *clb5 ccd4*, still falling short of levels in L*er*^{NFZ} (Figure 3c). Collectively, even though gene expression patterns in *clb5*^{NFZ} and *clb5*^{vLL} are not restored precisely to levels seen in L*er*^{NFZ}, the changes are sufficient to restore normal development.

The unique and strong induction of *PI* in response to the over-accumulation and subsequent cleavage of ZDS carotene substrates in *clb5* at 14 DPI was intriguing because potential AP3 and SEP3 regulators of *PI* in the ABCE model were not induced in *clb5* at this stage of development. Upon revisiting our RNA-sequencing data (Escobar-Tovar et al., 2020), it is clear *AP3* and *SEP3* were both significantly induced at 10 DPI (Figure S7). To confirm this result, *AP3* and *SEP3* transcripts were also quantified via a quantitative real-time polymerase chain reaction (qRT-PCR) in *clb5* seedlings and compared to the albino control L*er*^{NFZ}, as well as revertants *clb5 ccd4* and *clb5*^{NFZ}, at 10 DPI (Figure 4). At this time *AP3* was

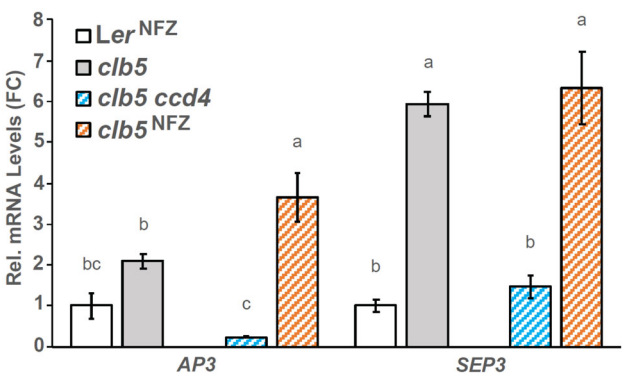

Figure 4. AP3 and SEP3 induction at 10 DPI precedes chimeric floral organ emergence.
Floral homeotic transcription factors *AP3* and *SEP3* mRNA levels in *clb5* and revertants, *clb5 ccd4* and *clb5*^{NFZ}, relative to L*er*^{NFZ}. In all experiments $n = 4$, each in triplicate. Statistical significance was determined based on FDR < 0.05. Data are represented as the mean ± SEM from four independent biological replicates.

© 2023 The Authors.

1365313x, 2023, 4, Downloaded from https://onlinelibrary.wiley.com/doi/10.1111/tpj.16168 by E.N.E.A., Wiley Online Library on [09/02/2024]. See the Terms and Conditions (https://onlinelibrary.wiley.com/terms-and-conditions) on Wiley Online Library for rules of use; OA articles are governed by the applicable Creative Commons License

induced by approximately two-fold and *SEP3* showed stronger induction of approximately six-fold compared to L*er*^{NFZ}. Similar to the RNA-sequencing data (Escobar-Tovar et al., 2020) the expression of *AP3* and *SEP3* was comparable to L*er*^{NFZ} in the *clb5 ccd4* revertant (Figure 4). Unexpectedly, transferring *clb5* seedlings to media containing NFZ at 5 DPI did not return *AP3* and *SEP3* expression back to the levels reported for L*er*^{NFZ}, and this is consistent with their elevated transcripts observed in 14 DPI seedlings undergoing the same treatment (Figures 4 and 3c).

The targeted gene expression analysis demonstrates that the accumulation and subsequent cleavage of ζ-carotenes isomers in *clb5* results in a broad reprogramming of gene regulatory networks crucial to FM identity (Figure 3). Furthermore, the induction of *PI* and detectable levels of transcripts for all other necessary MADS-box transcription factors in the ABCE model at 14 DPI, along with the earlier induction of *AP3* and *SEP3* at 10 DPI, appears to be sufficient for the promotion of chimeric flower organ development in the *clb5* seedlings (Figures 3 and 4). That said, the variability in the reversion of the *clb5*-associated transcriptional modulations observed across each of the revertants adds a level of complexity to the regulation of this phenomenon and is reminiscent of the partial complementarity of enzymatic and non-enzymatic contributions to carotenoid isomerisation in different tissues and light regimes (Beltran et al., 2015; Fantini et al., 2013; Isaacson et al., 2002; Park et al., 2002).

Development of chimeric floral organs in *clb5* requires flower-inducing long photoperiods in a GIGANTEA-independent manner

The premature FM initiation and termination of *clb5* is observed under long photoperiods (16:8 h light/dark), raising questions as to whether the early FM initiation is day-length dependent and, if so, does it require the GI and CO photoperiodic regulatory pathway. Premature FM initiation and termination (Figure 1) were consistently observed under long photoperiods with an approximate mean of three organs observed at 21 DPI, after which development ceased (Figure 5a,b). By contrast, *clb5* plants grown under short photoperiods (8:16 h light/dark) developed lamellar leaves (5.7 ± 0.2 leaves) with spiral phyllotaxy by 21 DPI, followed by an increase in the number of leaves (8.8 ± 0.4) by 28 DPI, and showed no sign of flower development (Figure 5a,b). The *gi-3* allele, which delays flowering under long photoperiods, was introduced into the *clb5* background (Figure 5c). The development of the *clb5 gi-3* double mutant was identical to that of *clb5* (Figure 5c). The lack of delay in FM formation in the *clb5 gi-3* double mutant indicates that *clb5* may be epistatic to or supersede GI.

Chimeric floral organ development in the *clb5* seedling requires functional AP1

The potential reliance of the *clb5*-associated transcriptional deregulation within the meristem on the well documented master regulators of FM identity, LFY and AP1, is intriguing. *clb5 lfy-4* and *clb5 ap1-3* double mutants were generated to explore this possibility, with *clb5 lfy-4* maintained as a double heterozygote given the homozygous lethality/sterility of both mutations. Out of 232 albino *clb5*$^{(-/-)}$ *lfy-4*$^{(+/-)}$ seedlings screened, it was anticipated that one quarter of the plants (i.e. 58 plants) should be homozygous for both mutations, consistent with the observed segregation of *lfy-4* plants in the soil grown green *clb5*$^{(+/-)}$ *lfy-4*$^{(+/-)}$ plants. However, all 232 plants homozygous for *clb5*$^{(-/-)}$ and segregating for *lfy-4*$^{(+/-)}$ were identical to *clb5*, with no reversion to normal leaf development or signs of indeterminacy observed (Figure 6a). By contrast, *clb5 ap1-3* seedlings differed from the single *clb5* mutant (Figure 6a). At 28 DPI, a majority (76%) of *clb5 ap1-3* seedlings displayed an enlarged meristem with no chimeric floral organs (Figure 6b,c). This inhibition of organ development is dependent on the over accumulation and subsequent cleavage of ZDS substrates, given that *ap1-3* grown on NFZ (*ap1-3*^{NFZ}), *clb5 ap1-3* seedlings transferred to NFZ at 5 DPI (*clb5 ap1-3*^{NFZ}) and *clb5 ap1-3* grown under low light (*clb5 ap1-3*^{vLL}) all developed similarly to the L*er*^{NFZ}, albeit with *ap1* mutant flowers (Figure S8a–c).

According to the observed *clb5 ap1-3* phenotypes, it appears that AP1 is not required for the transition of *clb5* to the FM, but is critical for chimeric floral organ development in *clb5*. To better understand the role of AP1 in the chimeric floral organ development of *clb5*, the transcriptional reprogramming in *clb5 ap1-3* at 14 DPI was explored (Figure 6d–f; Figure S8d). Consistent with the further enlarged meristem in *clb5 ap1-3*, *CLV3* was upregulated significantly, whereas *WUS* remained unchanged in *clb5 ap1-3* compared to *clb5* (Figure S8d). Regarding the AP2-like floral repressors, no significant change in the *clb5* associated repression of *SNZ*, *TOE1* and *TOE3* was observed in *clb5 ap1-3* (Figure 6d). Although the *ap1-3* mutation had no significant impact on floral promoting transcription factors *SOC1* and *FD*, *FUL* is repressed significantly in *clb5 ap1-3* seedlings compared to *clb5* (Figure 6e). Furthermore, although *SVP* remained unchanged, *TFL1* transcripts increased slightly in *clb5 ap1-3* relative to *clb5* (Figure 6e).

In relation to floral organ development, the A-, B-, C- and E-class gene expression profile is significantly altered in *clb5 ap1-3* compared to *clb5* (Figure 6f). Introduction of the *ap1-3* mutation manifests in a significant reduction in the B-class gene, *PI*, by more than 50% in *clb5 ap1-3* seedlings compared to *clb5* (Figure 6f). This is concurrent with an altered expression pattern among E-class genes.

© 2023 The Authors.

1365313x, 2023, 4, Downloaded from https://onlinelibrary.wiley.com/doi/10.1111/tpj.16168 by E.N.E.A., Wiley Online Library on [09/02/2024]. See the Terms and Conditions (https://onlinelibrary.wiley.com/terms-and-conditions) on Wiley Online Library for rules of use; OA articles are governed by the applicable Creative Commons License

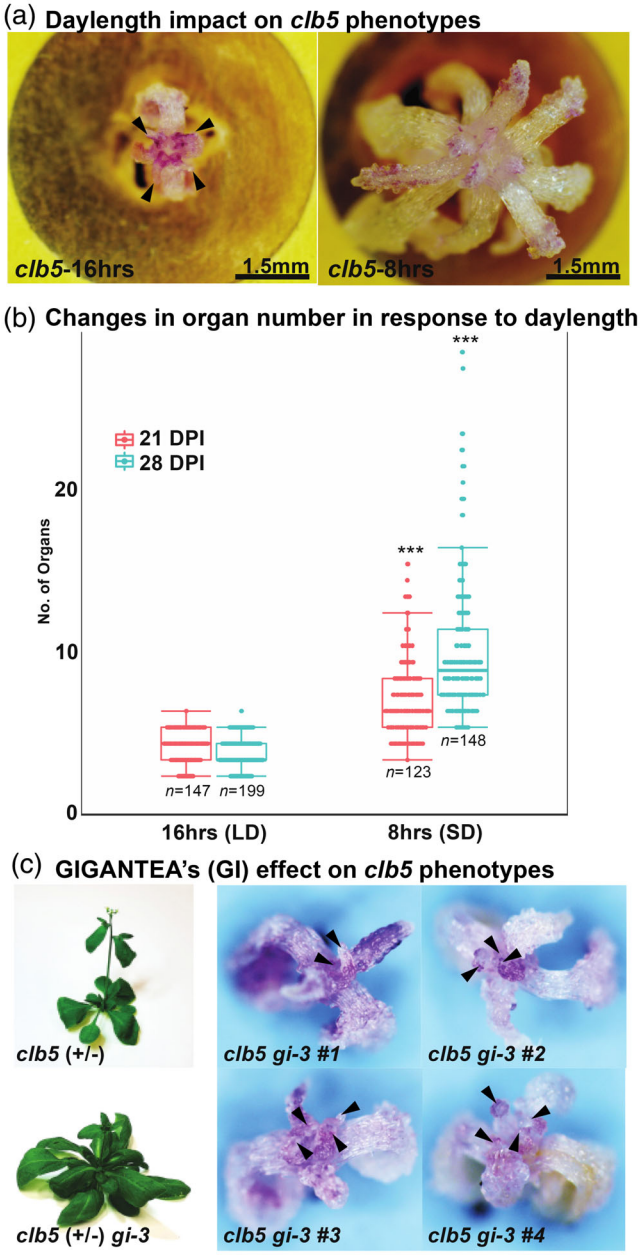

Figure 5. FM conversion in *clb5* requires long photoperiods in a GIGANTEA-independent manner.
(a) Dependence of *clb5* developmental phenotypes on daylength comparing of *clb5* seedlings grown under 16 hr (left) and 8 h (right) daylength (scale bar = 1.5 mm).
(b) Statistical analysis of the effect from daylength on *clb5* development according to number of organs developed post primary leaves at 21 and 28 DPI (***$P < 0.001$).
(c) Impact of the *gi-3* mutation on flowering time comparing soil grown *clb5*$^{(+/-)}$ and *clb5*$^{(+/-)}$ *gi-3* plants (left, two images) and developmental phenotypes in four representative albino *clb5 gi-3* seedlings displaying no change in chimeric floral organ development.
Chimeric floral organs in (a) and (c) are indicated by arrowheads.

SEP2 is significantly induced two-fold higher than L*er*^{NFZ} in *clb5 ap1-3*, whereas *SEP3* transcripts are almost undetectable (Figure 6f). The inability of *lfy-4* or *ap1-3* to restore the functional shoot apical meristem and normal leaf development in the *clb5* background combined with the restriction of the impact of *ap1-3* on the floral homeotic genes suggests that the *clb5*-associated FM identity is independent of and redundant to AP1, although AP1 is required for the subsequent floral organ development in *clb5* seedlings.

© 2023 The Authors.

1365313x, 2023, 4, Downloaded from https://onlinelibrary.wiley.com/doi/10.1111/tpj.16168 by E.N.E.A., Wiley Online Library on [09/02/2024]. See the Terms and Conditions (https://onlinelibrary.wiley.com/terms-and-conditions) on Wiley Online Library for rules of use; OA articles are governed by the applicable Creative Commons License

(a) ***clb5 lfy-4* and *clb5 ap1-3* phenotypes**

Green Plants (Soil Grown)	No. of plants w/ ... Wildtype (flowers)	Mutant (flowers)
clb5(+/-) *lfy-4*(+/-)	21	8
clb5(+/-) *ap1-3*(-/-)	0	29
Albino Plants (Media Grown)	**clb5-like (floral organs)**	**Reversion (leaves)**
clb5(-/-) *lfy-4*(+/-)	232	0
clb5(-/-) *ap1-3*(-/-)	312*	0

** indicates reduced floral organs in clb5 ap1-3*

(b) ***clb5 ap1-3*'s visual phenotypes**

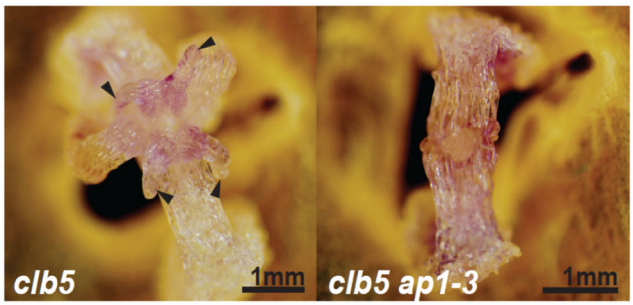

(c) ***ap1-3*'s effect on organ no.**

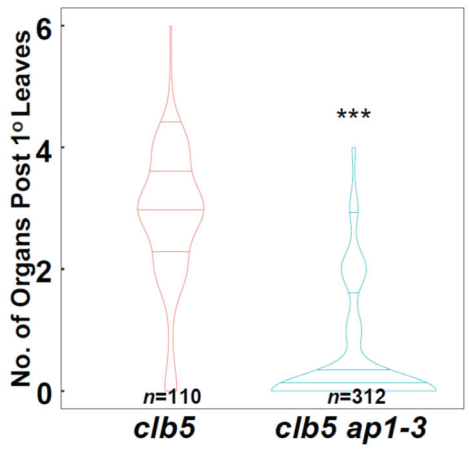

(d) **AP2-like floral repressing TFs**

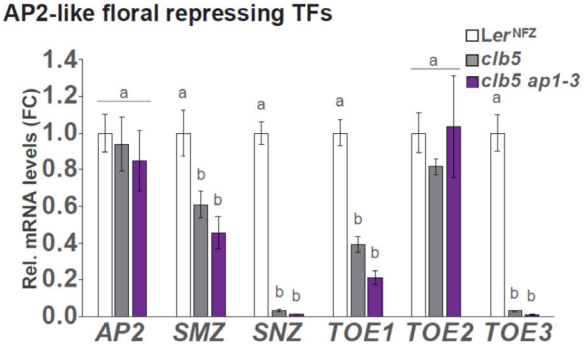

(e) **Floral promoting & meristem maintenance TFs**

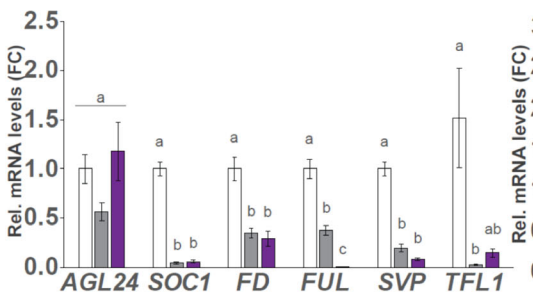

(f) **Floral homeotic TFs**

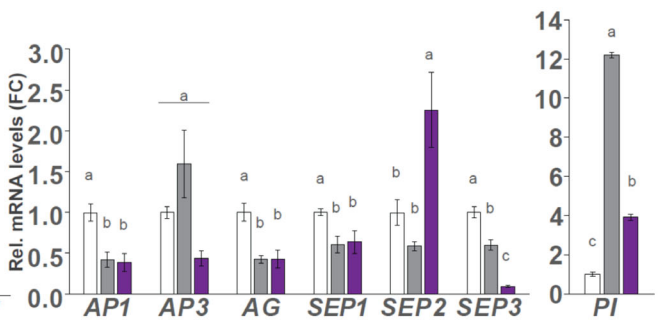

Figure 6. Chimeric floral organ development in *clb5* seedlings requires functional APETALA1.
(a) Table showing the segregation of the *lfy-4* homozygotes in soil grown green *clb5 lfy-4* F2 plants and the lack of reversion back to leaf development in the segregating albino *clb5 lfy-4* population, and the albino *clb5 ap1-3* double homozygous mutants.
(b) Statistical analysis of the effect from the *ap1-3* mutation on the development of *clb5* seedlings regarding number of organs developed post primary leaves at 28 DPI (***$P < 0.001$).
(c) Inhibition of chimeric floral organ development in *clb5 ap1-3* compared to *clb5* (scale bar = 1 mm).
(d–f) Transcript levels of AP2-like floral repressors (d), shoot apical meristem identity and floral promoting transcription factors (e) and floral homeotic transcription factors (f) relative to the albino control Ler^{NFZ} ($n \geq 3$, each in triplicate) (FDR < 0.05). Data are represented as the mean ± SEM.

AP1 guided repression of *ZDS* in stage 1–6 flowers of Arabidopsis supports the link between ζ-carotene accumulation and subsequent cleavage and regulation of FM identity, a critical regulation that is conserved in the sympodial tomato

Given previous evidence associating the over-accumulation and subsequent cleavage of ζ-carotene(s) with transition of the shoot apical meristem to a determinate FM, transcripts of carotenogenic genes in the poly-*cis*-transformation pathway were assessed through Arabidopsis flower development. Expression analysis of genes converting 15 *cis*-phytoene to *all trans*-lycopene was carried out over various stages of flower development (stages 1–6, 7–8, 9, 10, 11, 12 and 13b; as described in Smyth et al., 1990) in wild-type,

© 2023 The Authors.

1365313x, 2023, 4, Downloaded from https://onlinelibrary.wiley.com/doi/10.1111/tpj.16168 by E.N.E.A., Wiley Online Library on [09/02/2024]. See the Terms and Conditions (https://onlinelibrary.wiley.com/terms-and-conditions) on Wiley Online Library for rules of use; OA articles are governed by the applicable Creative Commons License

L*er*-0 and *ap1-1*, a null mutant of AP1 (Figure 7). The flower phenotypes of *ap1-1* demonstrate incomplete termination of the determinate FM consistent with disrupted FM identity, as well as altered floral organ development in the conversion of sepals to leaf-like bracts and an absence of petals consistent with a loss of an A-class floral homeotic transcription factor (Figure 7a). Given the dual roles of AP1 as a FM identity master regulator and a floral homeotic transcription factor, *ap1-1* was an ideal mutant to investigate the potential for floral specific regulation of carotenogenesis compared to wild-type. Furthermore, data available from AtGenExpress on the TAIR database (www.arabidopsis.org) provided preliminary evidence of an negative relationship between *ZDS* and *AP1* expression in flowers (Figure S9).

Over a flower developmental time course for both L*er*-0 and *ap1-1*, carotenoid biosynthetic gene expression was examined with the intention of identifying unique

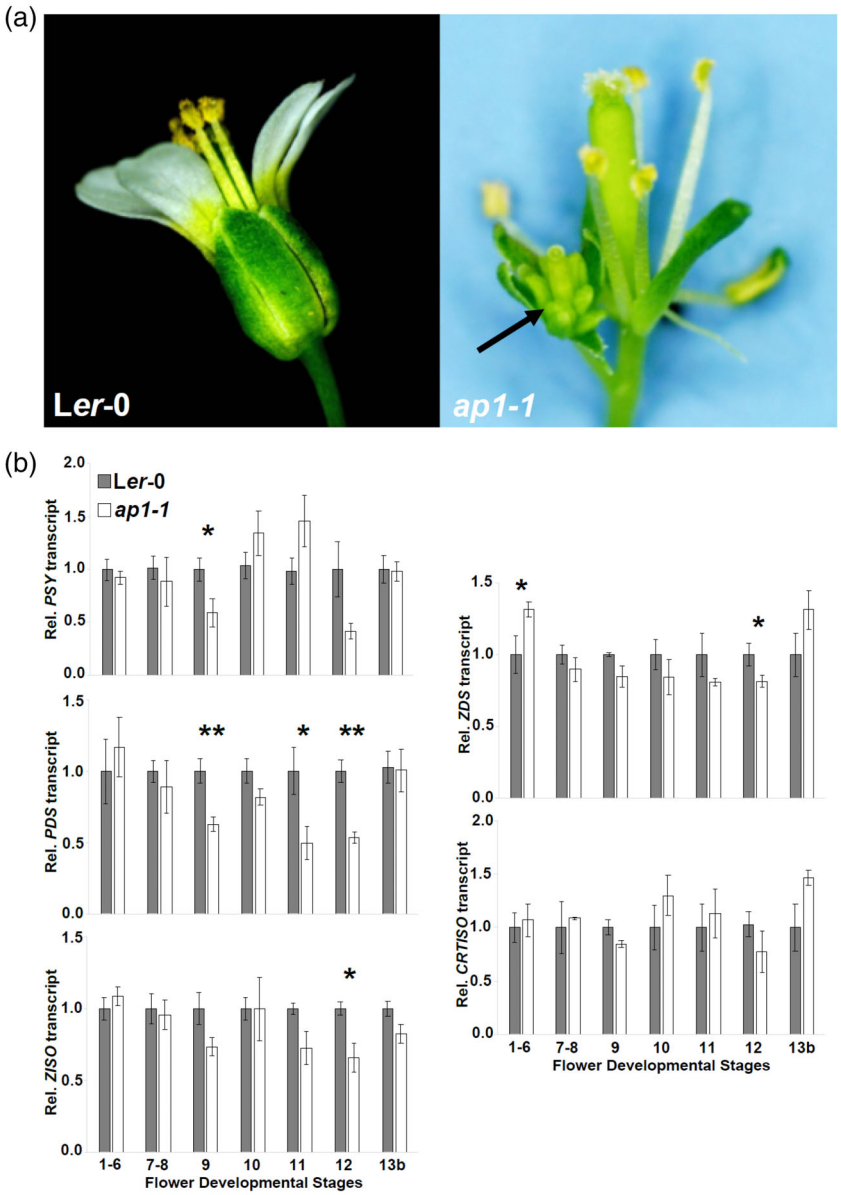

Figure 7. Unique repression of *ZDS* during in stage 1–6 flowers by APETALA1 supports the putative link between carotenoid biosynthesis and metabolism and regulation of FM identity.

(a) Developmental phenotypes in anthesis flowers of *ap1-1* (right) compared to wild-type L*er*-0 (left). The arrow indicates a secondary flower emerging as a result an indeterminate floral meristem in the *ap1-1* mutant.

(b) Stage specific comparison of carotenogenic transcript abundance in *ap1-1* (white) relative to L*er*-0 (gray). mRNA transcript levels were determined relative to wild-type (L*er*-0) at the same stage (*$P < 0.1$; **$P < 0.05$).

© 2023 The Authors.

1365313x, 2023, 4, Downloaded from https://onlinelibrary.wiley.com/doi/10.1111/tpj.16168 by E.N.E.A., Wiley Online Library on [09/02/2024]. See the Terms and Conditions (https://onlinelibrary.wiley.com/terms-and-conditions) on Wiley Online Library for rules of use; OA articles are governed by the applicable Creative Commons License

regulation of *ZDS* compared to other carotenogenic genes in early stages of FM identity and later in floral organ development (Figure 7b; Figure S9b). Through flower development transcript levels generally increase as development progresses for all genes in the poly-*cis*-transformation, as well as for PSY, the major rate-limiting enzyme of carotenogenesis, regardless of the AP1 function (Figure S9b). However, flower development stage specific comparisons between L*er*-0 and *ap1-1* demonstrated that carotenoid gene expression early in carotenogenesis is induced at stage 9 (i.e. *PSY* and *PDS*) and stage 12 (i.e. *PDS*, *ZISO* and *ZDS*) in an AP1-dependent manner (Figure 7b). More importantly, *ZDS* displays a unique AP1-dependent regulation in stages 1–6, during which FM identity is established and floral organ development is initiated (Figure 7b). *ZDS* transcripts are elevated approximately 30–40% in *ap1-1* flowers at stages 1–6 compared to L*er*-0, suggesting that AP1 actively represses *ZDS* accumulation in the initial stages of wild-type flower development in a direct or indirect manner (Figure 7b). By contrast, *CCD4* expression did not change in *ap1-1* at flower stage 1–6 compared to wild-type, but was substantially reduced throughout the remainder of flower development (Figure S10).

The AP1 guided repression of *ZDS* described above is consistent with the proposed role the accumulation of an ζ-carotene-derived apocarotenoid(s) plays in regulating FM identity. For further confirmation, available transgenic lines constitutively manipulating *ZDS* expression in tomato (i.e Arabidopsis *ZDS* over-expression, *AtZDS.OE*, and endogenous *ZDS* repression, *ZDS-RNAi*, lines) were assessed for aberrations in tomato FM identity and termination (McQuinn et al., 2020). Compared to the wild-type tomato, Ailsa Craig (AC), loss of the ζ-carotene-derived apocarotenoid(s) because of over-expression of *ZDS* in *AtZDS.OE* lines (*AtZDS.OE4.4* and *AtZDS.OE7.2*) resulted in significant increases in the development of compound inflorescences, similar to *ap1-1* in Arabidopsis, whereas *AtZDS.OE1A.1* and *AtZDS.OE9.1* narrowly missed the significance threshold ($P = 0.071$ and 0.097, respectively) (Figure 8). It should be mentioned that a low number of compound inflorescence were observed on the wild-type tomato plants, whereas *ZDS-RNAi* lines consistently showed no incidence of compound inflorescences (data not shown). These results in tomato confirm that the AP1-dependent repression of *ZDS* during the initial stages of floral development is integral in the regulation of FM identity and demonstrates a level of conservation across multiple plant species.

DISCUSSION

The present study elucidates a link between carotenoid biosynthesis/metabolism and the regulation of flower development, dependent on the massive reprogramming of gene regulatory networks deep within the meristem, establishing FM identity and function as observed in the Arabidopsis albino carotenogenic mutant *clb5*. In doing so, we exposed a redundant mechanism to establish FM identity initiated by AP1 and dependent on the E-class floral initiator and organ specification transcription factor, SEP3

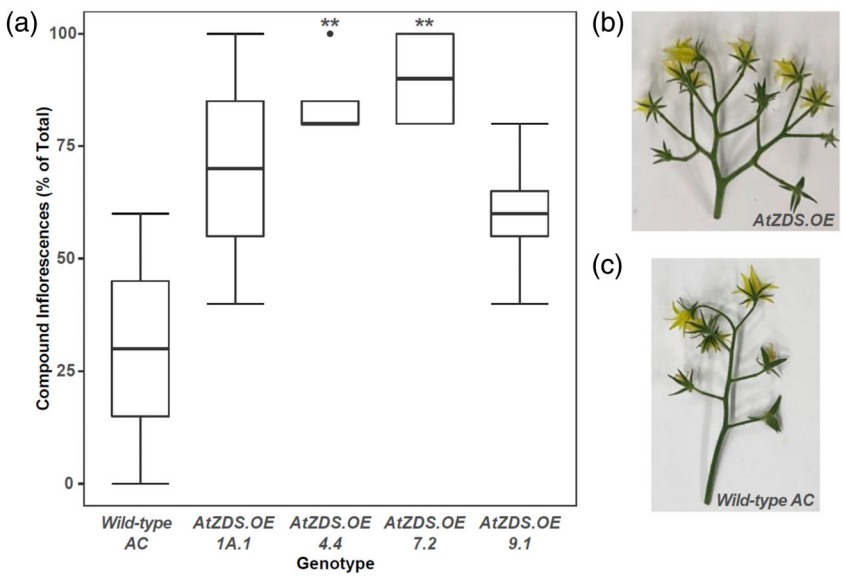

Figure 8. Increase incidence of compound inflorescences in *AtZDS.OE* lines of tomato compared to wild-type (AC) tomato plants.
(a) Percentage of compound inflorescences observed on wild-type (AC) and transgenic *ZDS* over-expression (*AtZDS.OE 1A.1, 4.4, 7.2, 9.1*) plants. Data collection was limited to the first five inflorescences on each plant, with each genotype represented as the mean ± SEM from four independent biological replicates. (**$P < 0.01$). (b) Representative inflorescence of *AtZDS.OE* lines. (c) Representative inflorescence of wild-type AC plants.

© 2023 The Authors.

1365313x, 2023, 4, Downloaded from https://onlinelibrary.wiley.com/doi/10.1111/tpj.16168 by E.N.E.A., Wiley Online Library on [09/02/2024]. See the Terms and Conditions (https://onlinelibrary.wiley.com/terms-and-conditions) on Wiley Online Library for rules of use; OA articles are governed by the applicable Creative Commons License

(Figure 9a). We further support this finding through manipulation of *ZDS* expression in transgenic tomato lines resulting in the disruption of FM identity and termination (Figure 9b,c). Our study exposes an additional layer of redundancy underpinning the regulation of flower development in Arabidopsis linked to the over-accumulation and subsequent cleavage of acyclic carotene substrates of ZDS, with evidence of conservation across multiple plant species.

The synthesis and identification of the causal apocarotenoid signal(s) in *clb5* remains complex and difficult to define

In depth analysis of *clb5*'s ζ-carotene profile exposed a complexity in the poly-*cis*-transformation of 15 *cis*-phytoene to *all trans*-lycopene not seen before, with 19 ζ-carotene isomers identified extending well beyond the seven ζ-carotene isomers previously identified in tomato fruit (Fantini et al., 2013; McQuinn et al., 2020). Impaired accumulation of the 19 ζ-carotene isomers upon chemical inhibition of PDS with NFZ restores close to normal leaf development and associated transcriptional deregulation in *clb5* seedlings, confirming that the floral developmental phenotypes of *clb5* can be attributed to the accumulation of these ζ-carotenes isomers, rather than a loss of downstream carotenoids or carotenoid-derived phytohormones (i.e. ABA and strigolactones), in agreement with our previous work (Avendaño-Vázquez et al., 2014).

The data accumulated so far suggest that enzymatic and/or non-enzymatic ζ-carotene cleavage is required to generate the apocarotenoid(s) that initiate the retrograde signaling cascade(s) driving the transcriptional reprogramming in *clb5*. It is possible that multiple ζ-carotene derivatives underpin the broad transcription reprogramming observed in *clb5*, similar to the complex array of strigolactones affecting different aspects of plant development and plant–microbe interactions (Al-Babili & Bouwmeester, 2015). Although the ability of CCD4 to cleave ζ-carotenes remains to be determined (Bruno et al., 2016), a role for CCD4 was of particular interest because of the reversion to normal leaf development and of a majority of genes transcriptionally deregulated in *clb5* previously reported in *clb5 ccd4* (Avendaño-Vázquez et al., 2014; Escobar-Tovar et al., 2020). In *clb5 ccd4* seedlings, increased levels of ten putative

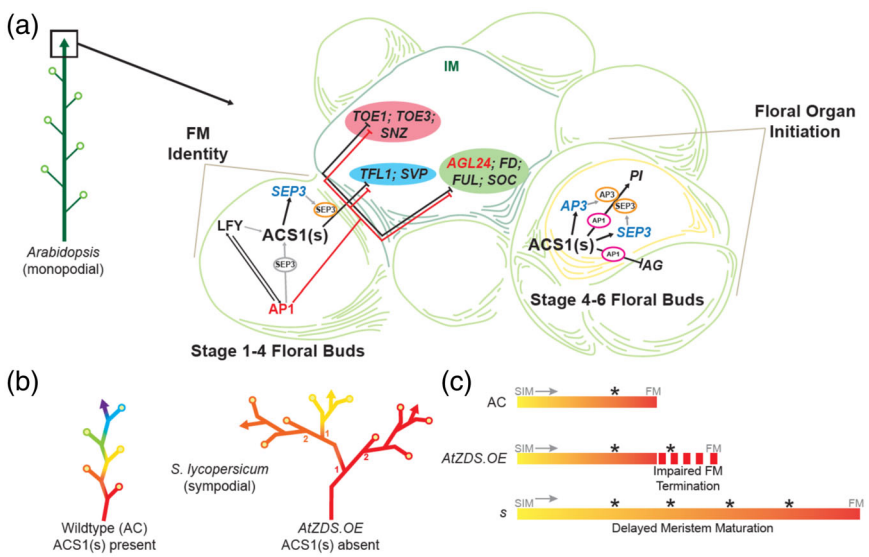

Figure 9. Summary of proposed link between carotenoid biosynthesis/metabolism and FM identity and floral organ initiation.
(a) In the monopodial Arabidopsis, the accumulation and subsequent cleavage of ζ-carotene isomers produces an unidentified apocarotenoid signal(s) identified as ACS1(s), which is involved in the regulation of FM identity (stage 1–4 floral buds) and floral organ initiation (stage 4–6 floral buds). FM Identity: the results demonstrate the role of AP1 in regulating ACS1(s) synthesis, whereas the available ChIP-seq data further indicate other FM identity master regulators LFY and SEP3 as potential additional regulators of ACS1(s) production. SEP3 is an early target of ACS1(s) in the *clb5* seedlings, the induction of which is hypothesized to facilitate downstream repression by ACS1(s) of AP2-like floral repressors (pink oval), with meristem maintenance (blue oval) and floral promoting (green oval) transcription factors restricting their expression to the inflorescence meristem (IM) and securing the determinate FM identity in the developing floral bud. Floral Organ Initiation: Early induction of *SEP3* and *AP3* as a result of ACS1(s) accumulation in *clb5* facilitates the strong induction of *PI* in an AP1-dependent manner enabling the initiation of the stamen primordia in stage 4–6 floral buds. In addition, ACS1(s) represses AG in an AP1-dependent manner.
(b) Visual diagram demonstrating how manipulation of ACS1(s) impacts inflorescence architecture in the sympodial tomato (*S.lycopersicum*) plant. Each represents a sympodial inflorescence meristem (SIM) that matures and transitions into a terminating FM (open circle). The arrows indicate the continuing progress of inflorescence development. The numbers on the compound inflorescence indicates the 1st and 2nd SIM that develop from the preceding SIM leading to a branched compound inflorescence architecture.
(c) Visual depiction of how the loss of ACS1(s) impairs sympodial floral development compared to wild-type (AC) and the *COMPOUND INFLORESCENCE* mutant, *s*, which delays SIM maturation and transition to the FM rather than impair FM identity and termination.

© 2023 The Authors.

1365313x, 2023, 4, Downloaded from https://onlinelibrary.wiley.com/doi/10.1111/tpj.16168 by E.N.E.A., Wiley Online Library on [09/02/2024]. See the Terms and Conditions (https://onlinelibrary.wiley.com/terms-and-conditions) on Wiley Online Library for rules of use; OA articles are governed by the applicable Creative Commons License

CCD4 ζ-carotene substrates were associated with a delay in the conversion to the FM and subsequent chimeric floral organ development. The observed delay in chimeric floral development in *clb5 ccd4* is linked to a minimal reversion of flower development associated genes deregulated in *clb5*, with only *WUS*, *CLV3* and *FUL* returning to control levels and *PI* and *AG* only partially recovering. That said, the *ccd4* mutation was able to revert the early induction of *AP3* and *SEP3* completely in the *clb5 ccd4* double mutant. Given the limited developmental reversion and small subset of genes restored in *clb5 ccd4*, it is likely the apocarotenoid signal(s) generated by CCD4-dependent ζ-carotene cleavage represents only a part of the ζ-carotene derived regulation of flower development.

Alternate means of apocarotenoid synthesis may also be required (i.e. non-enzymatic cleavage by $^1O_2$) (Escobar-Tovar et al., 2020; Hou et al., 2016) (Table S2). It is well documented that non-enzymatic cleavage provides some level of redundancy with enzymatic cleavage carried out by CCDs. This is a result of the capability of ROS to cleave randomly any, and all, unsaturated carbon–carbon double bonds on the carotenoid backbone, some of which are specific cleavage targets for CCD1, CCD4 and CCD7. Furthermore, ROS-mediated non-enzymatic cleavage is not restricted by limitations in active site size and shape and therefore can target any carotenoid available. In agreement, inferred reduction in random non-enzymatic ζ-carotene cleavage by $^1O_2$ under very low light conditions resulted in a complete reversion to normal leaf development associated with an increase in all 19 ζ-carotene isomers. A more comprehensive reversion of gene expression in *clb5*^{vLL} followed, with five genes (i.e. *SOC1*, *FD*, *TFL1*, *WUS* and *CLV3*) returned to control levels and seven genes (i.e. *SNZ*, *TOE1*, *TOE3*, *FUL*, *SVP*, *PI* and *AG*) partially restored, of which *FUL* was fully reverted and *PI* and *AG* were partially reverted in *clb5 ccd4*, demonstrating some level of redundancy (Figure 3; Table S2). These results partially explain the more complete reversion of *clb5*^{vLL} to normal leaf development and support a putative role of $^1O_2$ mediated non-enzymatic cleavage of ζ-carotenes in the *clb5* associated regulation of FM identity and floral organ development. Furthermore, non-enzymatic cleavage by light induced $^1O_2$ may represent just one step in a multistep synthesis of the causal apocarotenoid signal(s) similar to that of carotenoid derived hormones (i.e. ABA and strigolactone) and other apocarotenoid signals (i.e. anchorene). Alternatively, developmental reversion in *clb5*^{vLL} may reflect that light regime is altering other downstream elements involved in the *clb5* associated transcriptional reprogramming. Therefore, further investigation into potential roles of light intensity in ζ-carotene cleavage and the regulation of flower development in *clb5* is required.

Currently, the hypothesized synthesis of the ζ-carotene-derived apocarotenoid signals remains complex and difficult to define. Other CCDs (i.e. CCD1 and CCD7) and an unrelated lipoxygenase (LOX2) remain as potential candidates involved in the ζ-carotene-derived apocarotenoid synthesis associated with *clb5* developmental aberrations (Bruno et al., 2016; Gao et al., 2019; Sierra et al., 2022; Simkin et al., 2004). Indeed, considering the AP2-like floral repressors *SNZ*, *TOE1* and *TOE3* remained unchanged in *clb5 ccd4* and were only partially restored in *clb5*^{vLL}, it is plausible another carotenoid cleavage enzyme may be required for the synthesis of an additional causal apocarotenoid signal (s). Although the introduction of *ccd7* did not restore leaf development in our previous work, this may be a result of the stage of development that was analyzed (10 DPI, not 14 DPI) or may imply some level of redundancy (Avendaño-Vázquez et al., 2014). An exhaustive investigation into all CCDs and additional unrelated carotenoid cleavage enzymes (e.g. lipoxygenases) is required to better define the synthesis and identity of the ζ-carotene derived causal apocarotenoid signal(s) regulating FM identity and floral organ development in *clb5*.

A redundant mechanism to secure FM identity and function emerges in the *clb5* mutant linked to carotenoid biosynthesis and metabolism

We demonstrate that loss of ZDS in *clb5* mutant seedlings reprograms the shoot apical meristem from vegetative to reproductive development, producing a determinate FM from which whorled chimeric floral organs emerge. This altered meristematic function in *clb5* is accompanied by an accumulation of ζ-carotene isomers and results from the reprogramming of meristematic and FM identity gene regulatory networks closely mirroring the transcriptional regulation normally associated with AP1 activity (Kaufmann et al., 2010) (Figure 9a). The similarities are especially evident in the repression of the same three of six AP2-like transcription factors: *SNZ*, *TOE1* and *TOE3*. These three AP2-like transcription factors are directly repressed by AP1 in the early stages of FM emergence and development (Kaufmann et al., 2010) (Figure 9a). Furthermore, our analysis supports that the determinate FM in *clb5* seedlings may be established similar to AP1 through the repression of *TFL1* and the floral promoters *FD*, *SOC1* and *FUL* (Kaufmann et al., 2010) (Figure 9a). In the wild-type inflorescence meristem, TFL1 enhances indeterminate development by repressing *FUL*, *SEP1* and *SEP3* and restricting *LFY* and *AP1* expression to the FM, whereas SOC1, FD, FUL and AGL24 together promote the sequential emergence of floral primordia (Hanano & Goto, 2011). The direct repression by AP1 of *TFL1*, *SVP*, *SOC1*, *FD*, *FUL* and *AGL24* is required to ensure the determinate nature of the FM, as evidenced by the increased incidence of indeterminate compound flowers in the *ap1-1* mutant (Bowman et al., 1993; Kaufmann et al., 2010). This transcriptional regulation (minus *AGL24*) is largely mirrored in *clb5*

© 2023 The Authors.

1365313x, 2023, 4, Downloaded from https://onlinelibrary.wiley.com/doi/10.1111/tpj.16168 by E.N.E.A., Wiley Online Library on [09/02/2024]. See the Terms and Conditions (https://onlinelibrary.wiley.com/terms-and-conditions) on Wiley Online Library for rules of use; OA articles are governed by the applicable Creative Commons License

(Figure 9a). Therefore, given that the well-orchestrated transcriptional reprogramming by AP1 is critical in establishing Arabidopsis FM identity, it is likely that the reprogramming observed in *clb5* is also sufficient to establish FM identity in *clb5* seedlings (Bowman et al., 1993; Kaufmann et al., 2010).

By exploring floral development in the available transgenic tomato lines disrupting *ZDS* expression either by removing or increasing the levels of ζ-carotene-derived apocarotenoid signal(s) (i.e. through the over-expression or inhibition of *ZDS*, respectively) during early floral development, we further confirm the significance of this unique carotenogenic regulation in the establishment of FM identity and termination and suggest that this regulation is maintained in diverse species (Figure 9b,c). In both monopodial and sympodial plant species, FM termination is crucial in determining the floral architecture which has strong implications in crop yield. The monopodial Arabidopsis enabled the identification of the link between carotenogenesis and FM identity, which is sufficient to drive the transition from a vegetative meristem to a terminating FM. Furthermore, disruption of the gene regulatory networks targeted by the ζ-carotene derived apocarotenoid signal(s) results in compound inflorescences as indicated by *ap1-1* and *ap1-3* mutants in Arabidopsis (Bowman et al., 1993). This phenotype is shared in the null mutant *mc-vin* displaying a compound vegetative inflorescence (Yuste-Lisbona et al., 2016). Accordingly, MC is suggested to repress *SVP* and *AGL24* orthologues, *SINGLE FLOWER TRUSS* and *JOINTLESS*, respectively, to prevent the re-emergence of a vegetative meristem (Yuste-Lisbona et al., 2016).

In the sympodial tomato, the sympodial inflorescence meristem (SIM) goes through a maturation phase prior to terminating into a FM (Park et al., 2011). During this maturation phase, an additional SIM emerges, in a process that repeats on subsequent SIMs to establish a sequence of flowers and fruits on the tomato inflorescence (Figure 9b). Upon impairing FM termination by removing the ζ-carotene-derived apocarotenoid signal(s), in the case of *AtZDS.OE* tomato lines, additional SIMs emerge prior to FM termination generating compound inflorescences similar to the *s* mutant of tomato, but with a lower level of complexity (Figure 9b,c) (Park et al., 2011). A small percentage of these compound inflorescences is observed on and varies among wild-type tomato plants grown under the same conditions, suggesting that a level of sensitivity to environmental fluctuations may exist. Interestingly, increased ζ-carotene-derived apocarotenoid signal(s) accumulation in the case of *ZDS-RNAi* tomato lines eliminated the incidence of compound inflorescences, potentially removing this environmental regulation. Together, our results confirm a link between carotenogenesis and floral development, where the strict regulation of *ZDS* and associated transcriptomic reprogramming is both sufficient and required to regulate FM identity and termination with a level of conservation across plant species.

In *clb5*, the transition to the FM is achieved independent of AP1 activity. Furthermore, LFY is not required because no plants out of 232 examined displayed signs of normal leaf development or an indeterminate meristem in the *clb5 lfy-4* albino population homozygous for *clb5* and segregating for *lfy-4*. However, the role of CAL, a partially redundant paralog of AP1 in Arabidopsis (Bowman et al., 1993), has not been tested and remains an area for further investigation. It is unlikely that CAL is required given that, even with a functional CAL, the weaker allele of *ap1*, *ap1-3*, displays a reversion to indeterminacy in early FMs, whereas *cal* mutants do not display any floral phenotypes. Additionally, although the *cal* mutant does enhance *ap1* phenotypes in *ap1 cal* double mutant, information is limited regarding the direct transcriptional targets of CAL.

The SEP3 transcription factor is an interesting alternative, given its strong induction early in *clb5* development, and SEP3 transcriptional targets early in floral development (around stage 4) largely overlap with that of AP1 during the regulation of FM identity (Pajoro et al., 2014). SEP3 has been suggested to act as a pioneer transcription factor, similar to LFY (Jin et al., 2021; Wu et al., 2012), and delayed accumulation of LFY and SEP3 in the inflorescence meristem is suggested to be crucial for the prevention of precocious differentiation and termination of the floral meristem (Winter et al., 2011). Moreover, induction of *SEP3* in Arabidopsis results in transcriptional modulations similar to that observed in *clb5* plants; specifically, the early induction of *AP3*, delayed induction of *PI*, and the repression of *SOC1* and *SVP* transcription factors (Kaufmann et al., 2010). We hypothesize the induction of *SEP3* may signify an initial transcriptional regulation required for the premature transition to a terminating FM in *clb5* (Figure 9a). This is supported by the inability to return *SEP3* transcript levels back to that of $L{er}^{NFZ}$ upon transferring *clb5* plants to media contain NFZ at 5 DPI, suggesting that its induction occurs very early during *clb5* seedling development. Therefore, we propose that the reprogramming of gene regulatory networks initiated in *clb5* seedlings represents an alternative mechanism redundant to and independent of AP1 to safeguard the regulation of FM identity and reproductive success.

Unlike the establishment of the determinate FM, the subsequent formation of chimeric floral organs in *clb5* is dependent on AP1 activity (Figure 9a). The emergence and development of chimeric floral organs with stamenoid and carpelloid features is associated with a strong induction of the B-class MADS Box gene *PI* (Figure 9a). Although *PI* was the only floral homeotic gene from the ABCE model to be induced in *clb5* at 14 DPI, the detection of transcripts for all other floral homeotic genes, except *SEP4*, suggests that

© 2023 The Authors.

1365313x, 2023, 4, Downloaded from https://onlinelibrary.wiley.com/doi/10.1111/tpj.16168 by E.N.E.A., Wiley Online Library on [09/02/2024]. See the Terms and Conditions (https://onlinelibrary.wiley.com/terms-and-conditions) on Wiley Online Library for rules of use; OA articles are governed by the applicable Creative Commons License

the necessary MADS-box multimeric complexes were able to be formed. Furthermore, this chimeric floral organ development may also be dependent on an earlier induction of *SEP3* and *AP3* observed at 10 DPI (Figure 9a). This is supported by reports of *SEP3* induction resulting in a strong but delayed induction of *PI*, in combination with the observed reversion of *PI* transcript levels and loss of chimeric floral organs associated with an absence of *SEP3* transcription in the *clb5 ap1* double mutant at 14 DPI. Furthermore, although AP3 is not initially required for *PI* induction in the wild-type developing flower, AP3 is required for *PI* transcript maintenance (Goto et al., 1994). Therefore, we propose that, once the FM is established, the AP1 dependent induction of *PI* and subsequent chimeric floral organ initiation and development in *clb5* at 14 DPI is conditional on the induction of *SEP3* and *AP3* at 10DPI (Figure 9a).

The ζ-carotene associated conversion to the FM in *clb5* seedlings is dependent on long photoperiods and represents a redundant mechanism to safeguard FM identity and floral organ development potentially regulated by AP1 indirectly

The transition to flower development and ultimately the emergence of the FM requires both the accumulation of *FLOWERING LOCUS T* (*FT*) in the shoot apical meristem, which is heavily influenced by environmental factors (e.g. photoperiod and temperature) and the downstream induction of FM identity master regulators *AP1*, *LFY* and *CAULIFLOWER* (*CAL*) in the floral primordia, respectively (Andres & Coupland, 2012; Ferrandiz et al., 2000; Wils & Kaufmann, 2017). In that regard, it was expected similar requirements exist for the ζ-carotene associated conversion of the shoot apical meristem to the FM in *clb5* seedlings.

Extended photoperiods (16:8 h light/dark) promote *FT* expression through the GI and CO pathway driving the transition to reproductive development (Sawa et al., 2007; Tiwari et al., 2010; Valverde et al., 2004). This transition can be significantly delayed under short photoperiods (8:16 h light/dark) or if the GI/CO regulation of *FT* is disrupted by genetic mutation. Although short photoperiods inhibit the FM conversion of *clb5* and restore normal leaf development similar to L*er*^{NFZ}, GI was unnecessary for the induction of flowering by long photoperiods in *clb5*. Even though a decrease in day light hours may reduce the accumulation of light-induced $^1O_2$ in *clb5* seedlings, this reduction of $^1O_2$ is not considered sufficiently significant given our previous observations related to the severity of light reduction required to revert *clb5* developmental phenotypes and associated gene expression (Escobar-Tovar et al., 2020). This suggests that the FM-like transition in *clb5* seedlings is long photoperiod dependent and may be induced via *FT* regulation occurring either downstream of or epistatic to the GI and CO pathway. Alternatively, long photoperiods may also induce additional genetic factors requisite for downstream regulation of floral development and ζ-carotene associated regulation of FM identity independent of *FT*, as is the case for the meristematic transcription factor AGL24 (Torti et al., 2012 and Torti & Fornara, 2012). Regardless, further exploration into the requirement of long photoperiods and the potential dependence on *FT* accumulation earlier in *clb5* development will be paramount to define its role in the transition to flowering. Furthermore, given the hypothesized role of $^1O_2$ in the synthesis of the proposed mobile ζ-carotene-derived apocarotenoid(s), it is tempting to consider whether the transcriptional reprogramming may represent a means of triggering flowering in response to chloroplastic or abiotic stress under long photoperiods.

Chromatin immunoprecipitation-sequencing (ChIP-seq) analysis with SEP3, a direct transcriptional target of AP1, provides evidence of SEP3 binding near the *ZDS* locus early on in floral development, first observed at stage 4 (Pajoro et al., 2014). Importantly, this link between SEP3 and the poly-*cis*-transformation pathway of carotenogenesis is highly specific to *ZDS* because no SEP3 binding sites were identified near other genes in the pathway (i.e. *PDS*, *ZISO* and *CRTISO*) (Pajoro et al., 2014). As a master regulator, it remains plausible that AP1 may regulate the carotenogenic pathway within the FM as a redundant mechanism to safeguard FM identity and floral organ development. Indeed, AP1 uniquely regulates the poly-*cis*-transformation of 15-*cis*-phytoene to *all trans*-lycopene via the transcriptional repression of *ZDS* in stage 1–6 developing buds, when FM identity is established and floral organ development is initiated (Smyth et al., 1990). This regulation by AP1 is likely to be indirect given the lack of AP1 binding sites near the *ZDS* locus according to the available ChIP-seq data (Pajoro et al., 2014). Therefore, we propose that, in the early stages of floral development, AP1 promotes the redundant FM identity regulatory pathway observed in *clb5* through *SEP3* induction and subsequent SEP3 mediated repression of *ZDS* (Figure 9a). Moreover, the AP1-dependent indirect repression of *ZDS* early in floral development remains consistent with the deregulation of transcription factors involved in FM identity coinciding with ζ-carotene overaccumulation and cleavage in *clb5* mirroring the regulation by AP1 of FM identity in Arabidopsis.

Interestingly, *CCD4* was not regulated by AP1 during the establishment of the FM. However, *CCD4* is regulated by AP1 throughout the later stages of flower development. Similar to *ZDS*, *CCD4* does not appear to be a direct target of AP1, but rather may be indirectly regulated by AP1 through direct interaction with SEP3. Although *CCD4* does not seem to be induced by AP1 during the early stages of floral development, there is evidence that *CCD4* may be a direct target of and induced by LFY (Moyroud et al., 2011). All together, this suggests that carotenoid biosynthesis

© 2023 The Authors.

1365313x, 2023, 4, Downloaded from https://onlinelibrary.wiley.com/doi/10.1111/tpj.16168 by E.N.E.A., Wiley Online Library on [09/02/2024]. See the Terms and Conditions (https://onlinelibrary.wiley.com/terms-and-conditions) on Wiley Online Library for rules of use; OA articles are governed by the applicable Creative Commons License

and metabolism may be regulated by FM identity master regulators to safeguard and induce FM identity as observed in *clb5*.

The small but significant increase in *ZDS* transcripts observed in stage 1–6 developing flower buds of the *ap1-1* mutant compared to wild-type in Arabidopsis suggests that AP1-dependent indirect repression of *ZDS* in the developing wild-type flower may be under strict spatiotemporal regulation because these samples comprise a complex mixture of cell/tissue types. Such a restriction on *ZDS* repression would be advantageous for the protection of photosynthetic tissues in the developing flower, ensuring adequate biosynthesis of downstream photoprotective carotenoids and xanthophylls where required. That said, we propose that AP1-dependent repression of *ZDS* is constrained to the L2 layer of the FM where undifferentiated proplastids are considered to predominate (Charuvi et al., 2012). This localization is consistent with the role of AP1 in establishing FM identity during early stages of flower development and would limit negative impacts on photosynthetic tissues. Future high-resolution localization studies are essential to determine the exact spatiotemporal regulation of *ZDS* by AP1 and SEP3 at the point of floral primordia emergence and beyond.

CONCLUSIONS

Our data demonstrate a link between carotenoid biosynthesis and metabolism and the regulation of FM identity and function in Arabidopsis. The over-accumulation and subsequent cleavage of ζ-carotenes in *clb5* establishes FM identity redundant to and independent of AP1 under long photoperiods, whereas chimeric floral organ development in *clb5* remains dependent on functional AP1. Targeted transcriptomic analysis in the *clb5* mutant and revertant seedlings exposes a regulation of FM identity hypothesized to be conditional on the induction of SEP3, whih is based on the early strong induction of *SEP3* in *clb5* in combination with reports on the impacts of SEP3 manipulation and its transcriptional targets with respect to FM identity and function. Furthermore, investigation into the physiological relevance of the *clb5*-associated regulation of flower development has exposed a redundant regulatory mechanism to safeguard FM identity promoted by AP1 through its transcriptional upregulation of SEP3, as well as the subsequent interaction of SEP3 with the *ZDS* locus.

EXPERIMENTAL PROCEDURES

Plant materials and growth conditions

Wild-type (*Arabidopsis thaliana*, ecotype Landsberg *erecta*, L*er*-0), and *ccd4* (SALK_097984), *ap1-1* (CS28), *ap1-3* (CS6163), *gi-3* (CS51) and *lfy-4* (CS6274) mutant seeds, were obtained from Arabidopsis Biological Resource Center (abrc.osu.edu). Heterozygous *clb5* seeds were provided by Professor Patricia Leon (Universidad Nacional Autónoma de México, Cuernavaca, Mexico). YJ-STIG::GUS and SHP1::GUS seeds, previously described in Alvarez et al. (2009) were acquired from Professor John L. Bowman (Monash University, Melbourne, VIC, Australia). Mature green plants were grown on Seed Raising mix (Debco, Australia) with Osmocote™ Exact Mini (1 g kg^{-1}) (Scotts, Australia) for crosses and bulking seeds. All albino single and double mutant seedlings were grown on 1/2× MS medium (Caisson Laboratories, Inc., Smithfield, UT, USA) with Gamborg B-5 vitamins (PhytoTechnology Laboratories, Lenexa, KS, USA), supplemented with 3%(w/v) sucrose and solidified with 0.6%w/v phytoagar under white light (125 μmol m^{-2} sec^{-1}) and long day conditions (16:8 h light/dark), unless otherwise noted. Wild-type L*er*-0 seedlings grown on the above 1/2× MS media supplemented with 15 μM Norflurazon represent albino control plants. Wild-type (AC) and third generation (T_3) transgenic (*AtZDS.OE* and *ZDS-RNAi*) tomato plants were grown as described in McQuinn et al. (2020). The first five inflorescences on each plant were assessed and the presence of compound inflorescences was documented.

DNA isolation

Genomic DNA from Arabidopsis plants was isolated via a modified CTAB extraction method. Approximately 50–100 mg of fresh leaf tissue was homogenized with two 1/8″ steel ball bearings in 300 μL of CTAB buffer [2% (w/v) CTAB, 0.02 M EDTA, 1.4 M NaCl, 0.1 M Tris–HCl pH 8.0; preheated at 65°C] using a TissueLyser® (Qiagen, Hilden, Germany) for 1 min, and incubated for 30 min. Once samples were cooled to room temperature, 300 μL of chloroform was added, samples were vortexed thoroughly and the aqueous and organic phases were separated upon centrifugation at 8000 *g* for 30 min. Genomic DNA in the aqueous phase was precipitated in 300 μL of ice cold 100% isopropanol and subsequently washed with 500 μL of 70% ethanol. Air dried genomic DNA pellets were resuspended in Milli-Q water (Millipore Corp., Burlington, MA, USA) and diluted for subsequent genotyping.

Double mutant generation and genotyping

All *clb5* mutant seed stocks were maintained as heterozygous because of the homozygous lethality associated with the mutation. Heterozygous plants were selected based on a CAPS marker analysis with primers, *clb5*-For and *clb5*-Rev (Table S3) and the *Bam*HI restriction enzyme (Avendaño-Vázquez et al., 2014). The *clb5 ccd4* double mutant was generated via a cross with *ccd4* (SALK_097984) and backcrossed three times. Positive *ccd4* mutants were selected using gene specific primers *CCD4*-For and *CCD4*-Rev, in combination with the SALK insert primer BP-LBb1.3 (Table S3) (Alonso et al., 2003). Positive *clb5 gi-3* and *clb5 ap1-3* double mutants were selected based on clear morphological phenotypes (Araki & Komeda, 1993; Bowman et al., 1993) and confirmed via sequencing with primers *gi-3*_For and *gi-3*_Rev, and *ap1-3*_For and *ap1-3*_Rev, respectively (Table S3).

RNA extraction and quantitative RT-PCR analysis

Total RNA was isolated using a modified protocol from the RNeasy Minikit (Cat. No. 74106; Qiagen) as described in McQuinn et al. (2020). A qRT-PCR was performed using the Power SYBR® Green RNA-to-C_T™ 1-Step Kit (Cat No. 4309169; Applied Biosystems, Waltham, MA, USA) in a 5-μL reaction volume (2.5 μL of 2× Master Mix; 1 μM forward and reverse primers; 1 μl of total RNA; 0.46 μl of diethyl pyrocarbonate-treated water; 0.04 μl of RT enzyme mix). All genotypes and treatments were represented by a minimum of three biological replicates, each with triplicate technical replicates. Gene specific primers were checked for efficiency

© 2023 The Authors.

1365313x, 2023, 4, Downloaded from https://onlinelibrary.wiley.com/doi/10.1111/tpj.16168 by E.N.E.A., Wiley Online Library on [09/02/2024]. See the Terms and Conditions (https://onlinelibrary.wiley.com/terms-and-conditions) on Wiley Online Library for rules of use; OA articles are governed by the applicable Creative Commons License

using reference RNA composed of equal volume of RNA from each genotype and treatment (for primer sequences, see Table S3). A standard curve was included on each plate for the specific gene being analyzed using reference RNA (serial dilutions: 50, 5, 0.5, 0.05 and 0.005 ng) in triplicate. For each gene analysis, template-free and negative-RT controls were included. RT-PCR reactions were carried out using a LightCycler® 480 System (Roche, Basel, Switzerland) under the following reaction conditions: reverse transcription at 48°C for 30 min; enzyme activation at 95°C for 10 min; followed by 40 cycles of 95°C for 15 sec and 60°C for 1 min. A dissociation curve was added at the end of the run for verification of primer specificity.

Software provided with the LightCycler® 480 instrument (Roche) was used to determine gene specific threshold cycles (C_T) including the endogenous reference (18S rRNA) for every sample. C_T values were extracted and the standard curve method was applied to calculate relative mRNA levels in comparison to the albino control (L*er*^{NFZ}).

Cryo-SEM

Seedling and flower samples were mounted on a metal sample holder with a conductive adhesive [mixture of Tissue-Tek OCT (Sakura Finetek Japan Co., Ltd, Tokyo, Japan) and colloidal graphite] and then snap frozen by plunging into a LN_2 slush. Samples were subsequently transferred through the CRYO preparation chamber (Oxford CT1500; Oxford Instruments, Abingdon, UK) to the CRYO stage on a field emission gun SEM (model 4300; Hitachi, Tokyo, Japan) for etching. Here, unwanted frost was sublimated from the frozen sample surface at −90°C. After etching, the sample was transferred to the CRYO preparation chamber and sputter coated with Au at ~5 mA at near LN_2 temperature. After coating, the sample was transferred back onto the SEM CRYO stage for observation at 3.0 kV accelerating voltage using a secondary electron detector and Hitachi SEM software.

Histochemical GUS staining

Intact Arabidopsis flowers and seedlings were first fixed in ice cold 90% acetone under vacuum for 10 min and incubated at room temperature for 30 min. Flowers and seedlings were subsequently incubated in staining buffer (50 mM $NaPO_4$ pH 7.2, 0.5% Triton X-100, 10 mM EDTA), 2 mM potassium ferrocyanide [$K_4F_3(CN)_6$], 2 mM potassium ferricyanide [$K_3Fe_3(CN)_6$:H_2O] under vacuum for 15 min, and then incubated again in staining buffer containing 2 mM 5-bromo-4-chloro-3-indolyl-beta-D-glucuronic acid (X-gluc) on ice, under vacuum for 20 min, three times. Tissue samples were then incubated at 37°C in staining buffer with X-gluc overnight or until the blue precipitate (dichloro-dibromoindigo) was observed. Chlorophyll was extracted by washing with 70% ethanol. Samples were stored in 70% ethanol. Images of GUS staining in the flowers and seedlings were acquired using an SZX16 stereomicroscope (Olympus, Tokyo, Japan).

Carotenoid separation and quantification

Carotenoids were extracted in the dark from ~50 mg of ground *clb5* seedlings grown under standard (125 μmol m^{-2} sec^{-1}) or low light (<10 μmol m^{-2} sec^{-1}) with 360 μL of ethyl acetate:acetone (3:2 v/v) and separated with 240 μL Milli-Q water. The upper phase was transferred to a new tube and dried down under nitrogen gas. Carotenoids were resuspended in 45 μL of 100% ethyl acetate in preparation for separation and quantification by HPLC. HPLC analysis was carried out as described previously (McQuinn et al., 2020). All solvents used were HPLC grade. There was a minimum of three replicates per genotype and treatment.

ζ-Carotene isomer identification via LC-APCI-HRMS

Carotenoid extraction was performed as previously described (Fiore et al., 2012). Settings for HRMS equipped with an APCI source were as previously described (Diretto et al., 2019). ζ-carotene isomers were identified by comparing chromatographic and MS properties of each compound with the literature data for ζ-carotene and ζ-carotene-related compounds (Fantini et al., 2013) (http://carotenoiddb.jp), on the basis of the *m*/*z* accurate masses according to the Pubchem database for monoisotopic masses and on the basis of mass fragmentation in Metlin, or through the comparison between experimental and theoretical mass fragmentation, performed using MASSFRONTIER, version 7.0 (Thermo Fisher Scientific, Waltham, MA, USA).

Statistical analysis

Statistical analysis of carotenoid amounts (ng/μl) acquired via HPLC was carried out using unpaired two-sided Student's *t*-test comparing each carotenoid from a genotype/condition back to the corresponding carotenoid in *clb5* separately. $P < 0.05$ was considered statistically significant. An unpaired two-sided Student's *t*-test was also used to analyze the change in organ development between *clb5* and *clb5 ap1-3* (significance threshold, $P < 0.05$) and to determine significance of carotenoid biosynthetic gene specific qRT-PCR results for individual stages of flower development between the two genotypes, L*er*-0 and *ap1-1*. For the gene expression analysis, a significance threshold of $P < 0.1$ was applied because of the reduced number of biological replicates and increased variability related to limited tissue and staging strategy employed, respectively. Regarding transcriptomic analysis of flower development related genes in seedlings via qRT-PCR, for each comparison of gene transcript abundance between each genotype and/or condition, an ANOVA was performed to determine whether at least one of the genotypes and/or conditions was significantly different ($P < 0.05$). If satisfied, significantly different genotypes and/or conditions were identified using the least signiifcant difference with a FDR < 0.05.

ACCESSION NUMBERS

Germplasm: Wild-type *Arabidopsis thaliana*, ecotype Landsberg *erecta*, L*er*-0, CS20; *ccd4*, SALK_097984; *ap1*-1, CS28; *ap1-3*, CS6163; *gi-3*, CS51; and *lfy-4*, CS6274; Wild-type *Solanum lycopersicum*, Ailsa Craig, AC; *AtZDS.OE* lines 1A.1, 4.4, 7.2, and 9.1; *ZDS-RNAi* lines, 2.2 and 7.1. Genes: *PSY*, AT5G17230; *PDS*, AT4G14120; *ZISO*, AT1G10830; *ZDS*, AT3G04870; *CRTISO*, AT1G06820; *AP2*, AT4G36920; *SMZ*, AT3g54990; *SNZ*, AT2g39250; *TOE1*, AT2g28550; *TOE2*, AT5g60120; *TOE3*, AT5g67180; *AGL24*, AT4G24540; *SOC1*, AT2G45660; *FD*, AT4G35900; *FUL*, AT5G60910; *SVP*, AT2G22540; *TFL1*, AT5G03840; *AP1*, AT1G69120; *AP3*, AT3G54340; *PI*, AT5G20240; *AG*, AT4G18960; *SEP1*, AT5G15800; *SEP2*, AT3G02310; *SEP3*, AT1G24260.

ACKNOWLEDGEMENTS

We thank Melanie Rug, Hua Chen and the facilities of Microscopy Australia at the Advanced Imaging Precinct, Australian National University (a facility funded by the University and State and

© 2023 The Authors.

1365313x, 2023, 4, Downloaded from https://onlinelibrary.wiley.com/doi/10.1111/tpj.16168 by E.N.E.A., Wiley Online Library on [09/02/2024]. See the Terms and Conditions (https://onlinelibrary.wiley.com/terms-and-conditions) on Wiley Online Library for rules of use; OA articles are governed by the applicable Creative Commons License

Federal Governments) for their scientific guidance and technical assistance. We also thank Mary Byrne at University of Sydney for intellectual insight and John L. Bowman and Jose Alvarez at Monash University for their contribution of seeds for the YJ-STIG:GUS and SHP1:GUS lines. This research was funded by the Australian Research Council Centre of Excellence for Plant Energy Biology, Grant Number: CE140100008 and Australian Research Council Laureate Fellowship, Grant Number: FL190100056 for BJP and Consejo Nacional de Ciencia y Tecnologia, Mexico (CB 220534) and DGAPA-UNAM (IN204617 and IN207320) for PL. Open access publishing facilitated by Australian National University, as part of the Wiley - Australian National University agreement via the Council of Australian University Librarians.

AUTHOR CONTRIBUTIONS

RPM, PL and BJP designed the experiments. RPM, LET, SF, JS, GD and JJG conducted the experiments. RPM, EJF, GD, PL and BJP analyzed the data. RPM, EJF, GD, PL and BJP wrote/edited the paper. RPM and JL prepared the figures. PL, GG and BJP supervised the research. All authors approved the final version of the manuscript submitted for publication.

CONFLICT OF INTEREST

The authors declare no conflict of interest.

SUPPORTING INFORMATION

Additional Supporting Information may be found in the online version of this article.

Figure S1. Complete flowers of L*er*^{NFZ} and wild-type flowering time.

Figure S2. Gibberellic acid treatment of *clb5* compared to *pds3*.

Figure S3. Floral tissue specific cell structures and carpel specific gene expression.

Figure S4. HPLC chromatograph displaying complex carotenoid profile of *clb5* seedlings.

Figure S5. Verification of ζ-carotene isomer identity in *clb5* seedlings by LC-APCI-HRMS.

Figure S6. Gene expression and histochemical analysis of *WUS* and *CLV3*.

Figure S7. *AP3* and *SEP3* transcript levels in *clb5* and *clb5 ccd4* compared to *pds3* according to RNA-sequencing analysis.

Figure S8. Phenotypic analysis and *WUS* and *CLV3* gene expression of *clb5 ap1-3*.

Figure S9. Regulation of carotenogenesis by AP1 in Arabidopsis flower development.

Figure S10. CCD4 expression through floral development in wild-type and *ap1-1* plants.

Table S1. HPLC-PDA-APCI-HRMS (+/−) summary of *clb5's* ζ-carotene profile.

Table S2. Alternative means of causal apocarotenoid signal(s) synthesis in *clb5*.

Table S3. Genotyping and Gene expression analysis primers.

REFERENCES

Al-Babili, S. & Bouwmeester, H.J. (2015) Strigolactones, a novel carotenoid-derived plant hormone. *Annual Review of Plant Biology*, **66**, 161–186.

Alonso, J., Stepanova, A.N., Leisse, T.J., Kim, C.J., Chen, H., Shinn, P. *et al.* (2003) Genome-wide insertion mutagenesis of *Arabidopsis thaliana*. *Science*, **301**, 653–657.

Alvarez, J.P., Goldshmidt, A., Efroni, I., Bowman, J.L. & Eshed, Y. (2009) The *NGATHA* distal organ development genes are essential for style specification in *Arabidopsis*. *The Plant Cell*, **21**, 1373–1393.

Andres, F. & Coupland, G. (2012) The genetic basis of flowering responses to seasonal cues. *Nature Genetics*, **13**, 627–639.

Araki, T. & Komeda, Y. (1993) Analysis of the role of the late-flowering locus, *Gl*, in the flowering of *Arabidopsis thaliana*. *The Plant Journal*, **3**, 231–239.

Avendaño-Vázquez, A.-O., Cordoba, E., Llamas, E., San Roman, C., Nisar, N., De la Torre, S. *et al.* (2014) An uncharacterized apocarotenoid-derived signal generated in ζ-carotene desaturase mutants regulates leaf development and the expression of chloroplast and nuclear genes in *Arabidopsis*. *The Plant Cell*, **26**, 2524–2537.

Beltran, J., Kloss, B., Hosler, J.P., Geng, J., Liu, A., Modi, A. *et al.* (2015) Control of carotenoid biosynthesis through a heme-based cis-trans isomerase. *Nature Chemical Biology*, **11**, 598–605.

Bowman, J.L., Alvarez, J., Weigel, D., Meyerowitz, E.M. & Smyth, D.R. (1993) Control of flower development in *Arabidopsis thaliana* by *APETALA1* and interacting genes. *Development*, **119**, 721–743.

Bowman, J.L., Drews, G.N. & Meyerowitz, E.M. (1991) Expression of the *Arabidopsis* floral homeotic gene *AGAMOUS* is restricted to specific cell types late in flower development. *The Plant Cell*, **3**, 749–758.

Bruno, M., Koschmieder, J., Wuest, F., Schaub, P., Fehling-Kaschek, M., Timmer, J. *et al.* (2016) Enzymatic study on AtCCD4 and AtCCD7 and their potential to form acyclic regulatory metabolites. *Journal of Experimental Botany*, **67**, 5993–6005.

Cazzonelli, C.I., Hou, X., Alagoz, Y., Rivers, J., Dhami, N., Lee, J. *et al.* (2020) A cis-carotene derived apocarotenoid regulates etioplast and chloroplast development. *eLife*, **9**, e45310.

Chan, K.X., Phua, S.Y., Crisp, P., McQuinn, R.P. & Pogson, B.J. (2016) Learning the languages of the chloroplast: retrograde signaling and beyond. *Annual Review of Plant Biology*, **67**, 25–53.

Chandler, J.W. (2012) Floral meristem initiation and emergence in plants. *Cellular and Molecular Life Sciences*, **69**, 3807–3818.

Charuvi, D., Kiss, V., Nevo, R., Shimoni, E., Adam, Z. & Reich, Z. (2012) Gain and loss of photosynthetic membranes during plastid differentiation in the shoot apex of *Arabidopsis*. *The Plant Cell*, **24**, 1143–1157.

Coen, E.S. & Meyerowitz, E.M. (1991) The war of the whorls: genetic interactions controlling flower development. *Nature*, **353**, 31–37.

D'Alessandro, S., Mizokami, Y., Legeret, B. & Havaux, M. (2019) The apocarotenoid β-cyclocitric acid elicits drought tolerance in plants. *iScience*, **19**, 461–473.

Dickinson, A.J., Lehner, K., Mi, J., Jia, K.-P., Mijar, M., Dinneny, J. *et al.* (2019) β-Cyclocitral is a conserved root growth regulator. *Proceedings of the National Academy of Sciences of the United States of America*, **116**, 10563–10567.

Diretto, G., Frusciante, S., Fabbri, C., Schauer, N., Busta, L., Wang, Z. *et al.* (2019) Manipulation of β-carotene levels in tomato fruits results in increased ABA content and extended shelf life. *Plant Biotechnology Journal*, **18**, 1185–1199.

Ditta, G., Pinyopich, A., Robles, P., Pelaz, S. & Yanofsky, M.F. (2004) The *SEP4* gene of *Arabidopsis thaliana* functions in floral organ and meristem identity. *Current Biology*, **14**, 1935–1940.

Escobar-Tovar, L., Sierra, J., Hernandez-Munoz, A., Mathioni, S., Cordoba, E., McQuinn, R.P., Meyers, B.C., Pogson, B.J. & Leon, P. (2020) Deconvoluting ACS1 retrograde signaling networks that regulate leaf development. *Plant Journal*, **105**(6), 1582–1599.

Fantini, E., Falcone, G., Frusciante, S., Giliberto, L. & Giuliano, G. (2013) Dissection of tomato lycopene biosynthesis through virus-induced gene silencing. *Plant Physiology*, **163**, 986–998.

Ferrandiz, C., Gu, Q., Martienssen, R. & Yanofsky, M.F. (2000) Redundant regulation of meristem identity and plant architecture by FRUITFULL, APETALA1 and CAULIFLOWER. *Development*, **127**, 725–734.

Fiore, A., Dall'Osto, L., Cazzaniga, S., Diretto, G., Giuliano, G. & Bassi, R. (2012) A quadruple mutant of *Arabidopsis* reveals a β-carotene hydroxylation activity for LUT1/CYP97C1 and a regulatory role of xanthophylls on determination of the PSI/PSII ratio. *BMC Plant Biology*, **12**, 50.

Gao, L., Gonda, I., Sun, H., Ma, Q., Bao, K., Tieman, D.M. *et al.* (2019) The tomato pan-genome uncovers new genes and a rare allele regulating fruit flavor. *Nature Genetics*, **51**, 1044–1051.

© 2023 The Authors.
The Plant Journal published by Society for Experimental Biology and John Wiley & Sons Ltd.,

1365313x, 2023, 4, Downloaded from https://onlinelibrary.wiley.com/doi/10.1111/tpj.16168 by E.N.E.A., Wiley Online Library on [09/02/2024]. See the Terms and Conditions (https://onlinelibrary.wiley.com/terms-and-conditions) on Wiley Online Library for rules of use; OA articles are governed by the applicable Creative Commons License

Goto, K. & Meyerowitz, E.M. (1994) Function and regulation of the *Arabidopsis* floral homeotic gene *PISTILLATA*. *Genes and Development*, **8**, 1548–1560.

Grandi, V., Gregis, V. & Kater, M.M. (2012) Uncovering genetic and molecular interactions among floral meristem identity genes in *Arabidopsis*. *The Plant Journal*, **69**, 881–893.

Gregis, V., Sessa, A., Colombo, L. & Kater, M.M. (2008) *AGAMOUS-LIKE24* and *SHORT VEGETATIVE PHASE* determine floral meristem identity in *Arabidopsis*. *The Plant Journal*, **56**, 891–902.

Hanano, S. & Goto, K. (2011) *Arabidopsis* TERMINAL FLOWER1 is involved in the regulation of flowering time and inflorescence development through transcriptional repression. *The Plant Cell*, **23**, 3172–3184.

Hong, M. (1998) To be, or not to be, a flower – control of floral meristem identity. *Trends in Genetics*, **14**, 26–32.

Hou, X., Rivers, J., Leon, P., McQuinn, R.P. & Pogson, B.J. (2016) Synthesis and function of apocarotenoid signals in plants. *Trends in Plant Science*, **21**, 792–803.

Isaacson, T., Ronen, G., Zamir, D. & Hirschberg, J. (2002) Cloning of *tangerine* from tomato reveals a carotenoid isomerase essential for the production of b-carotene and xanthophyll in plants. *The Plant Cell*, **14**, 333–342.

Jia, K.-P., Dickinson, A.J., Mi, J., Cui, G., Kharbatia, N.M., Guo, X. *et al.* (2019) Anchorene is carotenoid-derived regulatory metabolite required for anchor root formation in *Arabidopsis*. *Science Advances*, **5**, eaaw6787.

Jin, R., Klasfeld, S., Zhu, F., Garcia, M.F., Xiao, J., Han, S.-K. *et al.* (2021) LEAFY is a pioneer transcription factor and licenses cell reprogramming to floral fate. *Nature Communications*, **12**, 626.

Kaufmann, K., Wellmer, F., Muino, J.M., Ferrier, T., Wuest, S.E., Kumar, V. *et al.* (2010) Orchestration of floral initiation by APETALA1. *Science*, **328**, 85–89.

Krizek, B.A. & Fletcher, J.C. (2005) Molecular mechanisms of flower development: an armchair guide. *Nature Genetics*, **6**, 688–698.

Liebers, M., Grubler, B., Chevalier, F., Lerbs-Mache, S., Merendino, L., Blanvillain, R. *et al.* (2017) Regulatory shifts in plastid transcription play a key role in morphological conversions of plastids during plant development. *Frontiers in Plant Science*, **8**, 23.

Liljegren, S.J., Gustafson-Brown, C., Pinyopich, A., Ditta, G.S. & Yanofsky, M.F. (1999) Interactions among *APETALA1*, *LEAFY*, and *TERMINAL FLOWER1* specify meristem fate. *The Plant Cell*, **11**, 1007–1018.

MacAlister, C.A., Park, S.J., Jiang, K., Marcel, F., Bendahmane, A., Izkovich, Y. *et al.* (2012) Synchronization of the flowering transition by the tomato TERMINATING FLOWER gene. *Nature Genetics*, **44**, 1393–1398.

McQuinn, R.P., Gapper, N.E., Gray, A.G., Zhong, S., Tohge, T., Fei, Z. *et al.* (2020) Manipulation of ZDS in tomato exposes carotenoid- and ABA-specific effects on fruit development and ripening. *Plant Biotechnology Journal*, **18**, 2210–2224. Available from: https://doi.org/10.1111/pbi.13377

Molinero-Rosales, N., Jamilena, M., Zurita, S., Gomez, P., Capel, J. & Lozano, R. (1999) *FALSIFLORA*, the tomato orthologue of *FLORICAULA* and *LEAFY*, controls flowering time and floral meristem identity. *The Plant Journal*, **20**, 685–693.

Moyroud, E., Minguet, E.G., Ott, F., Yant, L., Pose, D., Monniaux, M. *et al.* (2011) Prediction of regulatory interactions from genome sequences using a biophysical model for the *Arabidopsis* LEAFY transcription factor. *The Plant Cell*, **23**, 1293–1306.

Pajoro, A., Madrigal, P., Muino, J.M., Matus, J.T., Jin, J., Mecchia, M.A. *et al.* (2014) Dynamics of chromatin accessibility and gene regulation by MADS-domain transcription factors in flower development. *Genome Biology*, **15**, R41.

Park, H., Kreunen, S.S., Cuttriss, A.J., DellaPenna, D. & Pogson, B.J. (2002) Identification of the carotenoid isomerase provides insight into carotenoid biosynthesis, prolamellar body formation, and photomorphogenesis. *The Plant Cell*, **14**, 321–332.

Park, S.J., Jiang, K., Schatz, M.C. & Lippman, Z.B. (2011) Rate of meristem maturation determines inflorescence architecture in tomato. *Proceedings of the National Academy of Sciences of the United States of America*, **109**, 639–644.

Pastore, J.J., Limpuangthip, A., Yamaguhi, N., Wu, M.-F., Sang, Y., Han, S.-K. *et al.* (2011) LATE MERISTEM IDENTITY2 acts together with LEAFY to activate *APETALA1*. *Development*, **138**, 3189–3198.

Pelaz, S., Ditta, G.S., Baumann, E., Wisman, E. & Yanofsky, M.F. (2000) B and C floral organ identity functions require *SEPALLATA* MADS-box genes. *Nature*, **405**, 200–203.

Pose, D., Yant, L. & Schmid, M. (2012) The end of innocence: flowering networks explode in complexity. *Current Opinion in Plant Biology*, **15**, 45–50.

Qin, G., Gu, H., Ma, L., Peng, Y., Deng, X.W., Chen, Z. *et al.* (2007) Disruption of phytoene desaturase gene results in albino and dwarf phenotypes in Arabidopsis by impairing chlorophyll, carotenoid, and gibberellin biosynthesis. *Cell Research*, **17**, 471–482.

Ramel, F., Birtic, S., Ginies, C., Soubigou-Taconnat, L., Triantaphylides, C. & Havaux, M. (2012) Carotenoid oxidation products are stress signals that mediate gene responses to singlet oxygen in plants. *Proceedings of the National Academy of Sciences of the United States of America*, **109**, 5535–5540.

Saddic, L.A., Huvermann, B., Bezhani, S., Su, Y., Winter, C.M., Kwon, C.S. *et al.* (2006) The LEAFY target LMI1 is a meristem identity regulator and acts together with LEAFY to regulate expression of *CAULIFLOWER*. *Development*, **133**, 1673–1682.

Sawa, M., Nusimov, D.A., Kay, S.A. & Imaizumi, T. (2007) FKF1 and GIGANTEA complex formation is required for day-length measurement in *Arabidopsis*. *Science*, **318**, 261–265.

Sierra, J., McQuinn, R.P. & Leon, P. (2022) The role of carotenoids as a source of retrograde signals: impact on plant development and stress responses. *Journal of Experimental Botany*, **73**, 7139–7154.

Simkin, A.J., Schwartz, S.H., Auldridge, M., Taylor, M.G. & Klee, H.J. (2004) The tomato *carotenoid cleavage dioxygenase 1* genes contribute to the formation of the flavor volatiles β-ionone, pseudoionone, and geranylacetone. *The Plant Journal*, **40**, 882–892.

Smyth, D.R., Bowman, J.L. & Meyerowitz, E.M. (1990) Early flower development in *Arabidopsis*. *The Plant Cell*, **2**, 755–767.

Tiwari, S.B., Shen, Y., Chang, H.-C., Hou, Y., Harris, A., Ma, S.F. *et al.* (2010) The flowering time regulator CONSTANS is recruited to the *FLOWERING LOCUS T* promoter via a unique *cis*-element. *The New Phytologist*, **187**, 57–66.

Torti, S. & Fornara, F. (2012) *AGL24* acts in concert with *SOC1* and *FUL* during *Arabidopsis* floral transition. *Plant Signaling & Behavior*, **7**, 1251–1254.

Torti, S., Fornara, F., Vincent, C., Andres, F., Nordstrom, K., Gobel, U. *et al.* (2012) Analysis of the *Arabidopsis* shoot meristem transcriptome during floral transition identifies distinct regulatory patterns and a leucine-rich repeat protein that promotes flowering. *The Plant Cell*, **24**, 444–462.

Valverde, F., Mouradov, A., Soppe, W., Ravenscroft, D., Samach, A. & Coupland, G. (2004) Photoreceptor regulation of CONSTANS protein in photoperiodic flowering. *Science*, **303**, 1003–1006.

Wang, J.Y., Haider, I., Jamil, M., Fiorilli, V., Saito, Y., Mi, J. *et al.* (2019) The apocarotenoid metabolite zaxinone regulates growth and strigolactone biosynthesis in rice. *Nature Communications*, **10**, 810.

Wellmer, F., Graciet, E. & Riechmann, J.L. (2014) Specification of floral organs in *Arabidopsis*. *Journal of Experimental Botany*, **65**, 1–9.

Wigge, P.A., Kim, M.C., Jaeger, K.E., Busch, W., Schmid, M., Lohmann, J.U. *et al.* (2005) Interation of spatial and temporal information during floral induction in *Arabidopsis*. *Science*, **309**, 1056–1059.

Wils, C.R. & Kaufmann, K. (2017) Gene-regulatory networks controlling inflorescence and flower development in *Arabidopsis thaliana*. *Biochimica et Biophysica Acta*, **1860**, 95–105.

Winter, C.M., Austin, R.S., Blanvillain-Baufume, S., Reback, M.A., Monniaux, M., Wu, M.F. *et al.* (2011) LEAFY target genes reveal floral regulatory logic, *cis* motifs, and a link to biotic stimulus response. *Developmental Cell*, **20**, 430–443.

Wu, M.-F., Sang, Y., Bezhani, S., Yamaguchi, N., Han, S.-K., Li, Z. *et al.* (2012) SWI2/SNF2 chromatin remodeling ATPases overcome polycomb repression and control floral organ identity with the LEAFY and SEPALLATA3 transcription factors. *Proceedings of the National Academy of Sciences of the United States of America*, **109**, 3576–3581.

Yuste-Lisbona, F.J., Quinet, M., Fernandez-Lozano, A., Pineda, B., Moreno, V., Angosto, T. *et al.* (2016) Characterization of *vegetative inflorescence* (*mc-vin*) mutant provides new insight into the role of *MACROCALYX* in regulating inflorescence development of tomato. *Scientific Reports*, **6**, 18796.

© 2023 The Authors.
The Plant Journal published by Society for Experimental Biology and John Wiley & Sons Ltd.,

1365313x, 2023, 4, Downloaded from https://onlinelibrary.wiley.com/doi/10.1111/tpj.16168 by E.N.E.A., Wiley Online Library on [09/02/2024]. See the Terms and Conditions (https://onlinelibrary.wiley.com/terms-and-conditions) on Wiley Online Library for rules of use; OA articles are governed by the applicable Creative Commons License